Ecotoxicology and Environmental Safety 216 (2021) 112180

Contents lists available at ScienceDirect

Ecotoxicology and Environmental Safety

journal homepage: www.elsevier.com/locate/ecoenv

Review

Atmospheric nitrogen deposition: A review of quantification methods and its spatial pattern derived from the global monitoring networks

Qi Zhang [a,b,1], Yanan Li [a,b,1], Mengru Wang [b], Kai Wang [a], Fanlei Meng [a], Lei Liu [c], Yuanhong Zhao [d], Lin Ma [e], Qichao Zhu [a], Wen Xu [a,*], Fusuo Zhang [a]

[a] College of Resources and Environmental Sciences; National Academy of Agriculture Green Development; Key Laboratory of Plant-Soil Interactions of MOE, China Agricultural University, Beijing 100193, China
[b] Water Systems and Global Change Group, Wageningen University & Research, P.O. Box 47, 6700 AA Wageningen, The Netherlands
[c] College of Earth and Environmental Sciences, Lanzhou University, Lanzhou 730000, China
[d] College of Oceanic and Atmospheric Sciences, Ocean University of China, Qingdao 266100, China
[e] Key Laboratory of Agricultural Water Resources, Hebei Key Laboratory of Soil Ecology, Center for Agricultural Resources Research, Institute of Genetic and Developmental Biology, Chinese Academy of Sciences, 286 Huaizhong Road, Shijiazhuang 050021, Hebei, China

ARTICLE INFO

Edited by: Professor Bing Yan

Keywords:
Atmospheric reactive nitrogen
Dry deposition
Wet deposition
Quantification methods
Monitoring networks

ABSTRACT

Atmospheric nitrogen (N) deposition is a vital component of the global N cycle. Excessive N deposition on the Earth's surface has adverse impacts on ecosystems and humans. Quantification of atmospheric N deposition is indispensable for assessing and addressing N deposition-induced environmental issues. In the present review, we firstly summarized the current methods applied to quantify N deposition (wet, dry, and total N deposition), their advantages and major limitations. Secondly, we illustrated the long-term N deposition monitoring networks worldwide and the results attained via such long-term monitoring. Results show that China faces heavier N deposition than the United States, European countries, and other countries in East Asia. Next, we proposed a framework for estimating the atmospheric wet and dry N deposition using a combined method of surface monitoring, modeling, and satellite remote sensing. Finally, we put forth the critical research challenges and future directions of the atmospheric N deposition.

Capsule: A review of quantification methods and the global data on nitrogen deposition and a systematic framework was proposed for quantifying nitrogen deposition.

1. Introduction

Over the last century, increased agricultural and industrial activities have dramatically influenced the global nitrogen (N) cycle, with global atmospheric reactive nitrogen (N_r) (NH_3 and NO_y) emissions estimated at 103 kg N yr^{-1} in the early-1990s and projected to double in 2050 (Galloway et al., 2004). The majority of emitted anthropogenic N_r components can enter terrestrial and marine ecosystems via atmospheric N deposition, a crucial component of the N cycle (Galloway et al., 2004; Fowler et al., 2015; Liu and Du, 2020). Excess N deposition can lead to a cascade of environmental problems, including soil acidification (Lu et al., 2014), water eutrophication of freshwater (Zhan et al., 2017), and reduction of biodiversity (Midolo et al., 2019). Over the past three decades, N_r emissions have been effectively controlled in Europe and the United States, as demonstrated by substantial declines in ambient N_r concentrations and deposition (Tørseth et al., 2012; Zhang et al., 2018). In contrast, N deposition did not markedly decrease and remained high in East Asia (especially in China) and India (Xu et al., 2015; Wen et al., 2020). Due to the dramatic increases in N-fertilizer use and fossil fuel combustion, NH_3 and NO_x emissions in China increased significantly between the 1980s and the 2010s. However, anthropogenic NO_x emissions began to decline after 2012 and were reduced by 59% in 2017 (22.0 Tg) relative to 2010 as the result of implementing stringent clean air actions, whereas NH_3 emissions remained stable in 2010–2017, approximately 10 Tg (X.D. Zheng et al., 2018; B. Zheng et al., 2018). Such high N_r emissions have attracted public concerns on air quality and its implications for N deposition in China (Liu et al., 2019; Yu et al., 2019) since high levels of N_r air concentrations and deposition is closely

* Corresponding author.
E-mail address: wenxu@cau.edu.cn (W. Xu).
[1] Contributed equally to this work.

https://doi.org/10.1016/j.ecoenv.2021.112180
Received 29 October 2020; Received in revised form 18 March 2021; Accepted 20 March 2021
Available online 14 April 2021

associated with ecological and human health (Abdolahnejad et al., 2018; Saki et al., 2019; Smith et al., 2000; Xu et al., 2018a).

Nitrogen deposition quantification is a prerequisite for formulating policies and management actions that reduce harmful effects on sensitive ecosystems and optimize N input to the agroecosystem. Many approaches have been developed to measure N deposition in different pathways, including wet N deposition, dry N deposition, and the total (wet plus dry) deposition (Pan et al., 2012; Xu et al., 2015). Wet N deposition can be readily determined with relatively high reliability (Wang et al., 2018). However, in the contexts of current changes in N_r emissions worldwide, its latest spatial pattern is still unknown. In addition, direct measurement of dry N deposition, especially at large spatial and temporal scales, remains a challenge due to various N_r species presented in gases- and particle-phase, particularly in remote regions (Vet et al., 2014).

Therefore, in this review, we systemically summarized the widely used N deposition quantification methods and wet N deposition fluxes from the global monitoring networks for the year 2017 to better understand the spatial pattern of wet N deposition worldwide. Besides, we proposed a comprehensive framework for estimating N deposition from a site to a regional or national scale. Finally, we discuss the research challenges and future directions of the atmospheric N deposition.

2. Influencing processes of atmospheric nitrogen deposition and research methods

2.1. Wet N deposition

All the processes of wet deposition are depicted in detail in Fig. 1. Wet N deposition refers to the gaseous and particulate N_r compounds in the atmosphere scoured to the Earth's surface by precipitation (rain or snow); it occurs via two processes: one is in-cloud scavenging (rainout), occurring when gases or particles are scavenged inside a cloud by cloud droplets, and the other is below-cloud scavenging (i.e., washout) via interception of gases and particulate matter (Seinfeld and Pandis, 2006). Furthermore, the N_r compounds may undergo chemical transformations during each one of the above processes. Note that most of the processes are reversible. For instance, the rain may scavenge particles below the cloud, but the raindrop generates new aerosols via the evaporation process (Fig. 1). Wet deposition fluxes of N_r species typically lie on the microphysics of the cloud and precipitation (e.g., nucleation scavenging during cloud formation, dissolution into aqueous droplets), which affects scavenging efficiencies of in-cloud and below-cloud processes, and the characteristics of different N_r species (e.g., NH_3, NO_2 and particulate ammonium (NH_4^+)) such as their concentrations, hygroscopicity/solubility, and particle size (X.D. Zheng et al., 2018; B. Zheng et al., 2018). It has been found that ammonium concentrations in cloud water dominate the total ammonium content in rainfall (Goncalves et al., 2003). When the NH_3 concentrations below the cloud level are much higher than that inside the cloud, the trend of NH_4^+ concentration in precipitation caused by in-cloud NH_3 scavenging will be altered by below-cloud scavenging (Mizak et al., 2005).

Wet deposition is usually determined via installing instruments in the open field to collect rain or snow for periods, usually ranging from several days to a month. Wet N deposition fluxes are the product of the measured N_r concentrations in precipitation and precipitation amount, using the following equations:

$$C_w = \sum_{i=1}^{n}(C_i P_i) \Big/ \sum_{i=1}^{n} P_i \quad (1)$$

where C_w is the volume-weighted mean concentration (mg N L^{-1}) calculated from the n precipitation samples within a month or a year, and the individual sample concentration C_i is weighted by the rainfall amount $_{Pi}$ for each sample.

$$D_w = P_t C_w / 100 \quad (2)$$

where D_w is the wet/bulk deposition flux (kg N ha^{-1}), P_t is the total amount of all precipitation events (mm), and 100 is a unit conversion factor.

Although it is relatively straightforward to quantify wet deposition, the uncertainties from the sampling, storage, and analysis methods still exist (Liu et al., 2015). A rain gauge (or open bucket) with a specific size is the commonly used samplers for measuring wet N deposition (Xu et al., 2015; Zhu et al., 2015). However, the resulting fluxes using this method should be defined as bulk N deposition (wet-only deposition

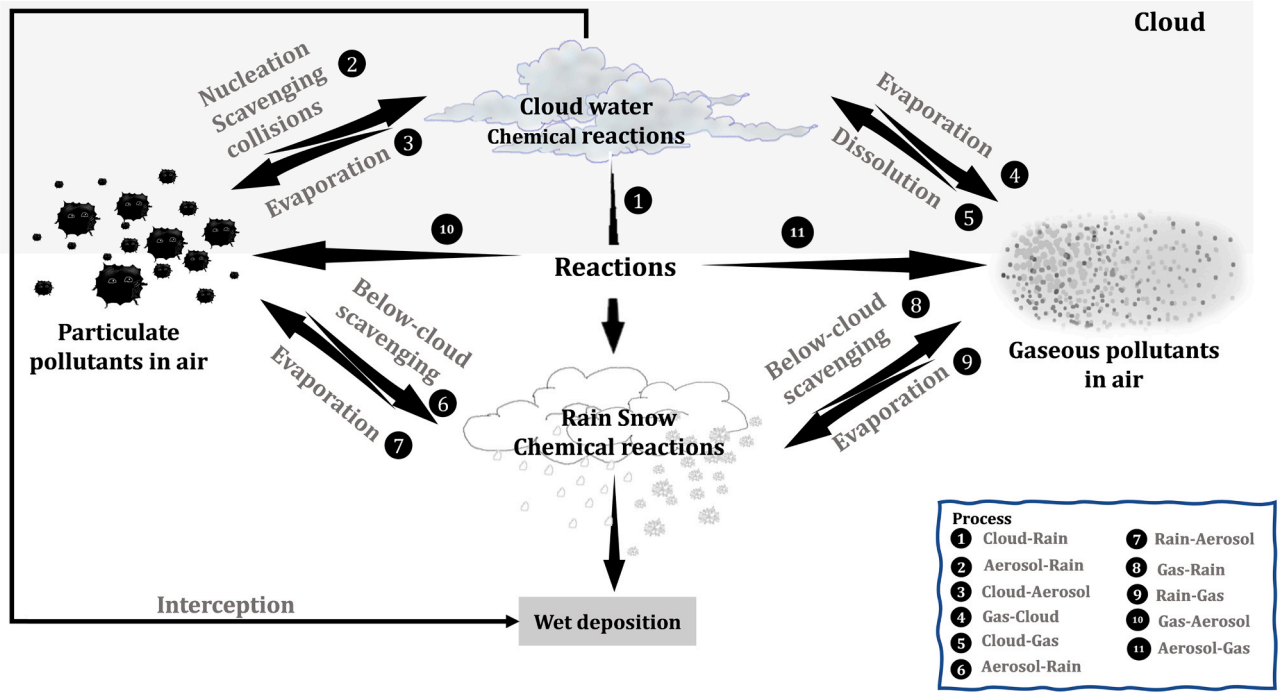

Fig. 1. Conceptual framework of wet deposition processes.

plus parts of dry-deposited gaseous and particulate N-compounds), which are higher than realistic wet N deposition (Dämmgen et al., 2005). For instance, the differences between bulk and wet-only N deposition were 1.3–9.6 kg N ha^{-1} yr^{-1} at three suburban and rural sites in the North China Plain, accounting for 5–32% of bulk deposition (Zhang et al., 2008). Such differences were equivalent to 12%−15% of the bulk deposition at four rural sites in southern China (Shen et al., 2013; Kuang et al., 2016; Song et al., 2017). A similar phenomenon was also reported in other regions worldwide, such as Greater Manchester (Lee and Longhurst, 1992), Connecticut (Nadim et al., 2001), and Belgium (Staelens et al., 2005). To perform an accurate wet deposition measurement, the wet-only samplers (as illustrated in Kuang et al., 2016) are recommended in future studies on N deposition quantification. Besides, short sampling periods (e.g., daily collection) and the addition of biocide and hydrochloric acid after sampling is recommended to avoid sample deterioration caused by bacterial action and NH_3 losses (Fattore et al., 2014; Xu et al., 2015; Izquieta-Rojano et al., 2016).

For bulk deposition or throughfall deposition in the forest ecosystem, the ion-exchange resin method is superior to conventional methods (i.e., traditional rainfall collection), which requires a lot of labor and expensive analytical costs implemented on a large scale (Fenn and Poth, 2004). This method was initially used to study forest soil N dynamics (Kjnaas, 1999), and more recently, it has been employed for quantifying N deposition in many studies (Hoffman et al., 2019). The ion-exchange resin method mainly measures NH_4^+, NO_2^-, and NO_3^- in N deposition but cannot determine wet organic N deposition in precipitation. The use of this method requires at least three KCl extractions to ensure the recovery efficiencies of ammonium nitrogen and nitrate nitrogen. Accurate quantification of N deposition is essential for better understanding the responses of ecosystems. The advantages and disadvantages of the methods for measuring wet and dry nitrogen deposition in arid and montane ecosystems in western North America have been introduced in detail in Fenn et al. (2009). Ochoa-Hueso et al. (2011) reviewed the ecological consequences of N deposition on the five Mediterranean regions of the world, and they found that California and the Mediterranean Basin are the most threatened by N deposition. Several forest ecosystem properties (e.g., soil acidification, plant biodiversity) in Europe and eastern North America are predicted to react with varying degrees of delay to the current pattern of decreasing N deposition (Gilliam et al., 2019; Schmitz et al., 2019).

2.2. Dry deposition

Nitrogen dry deposition refers to the process in which gaseous and particulate N_r components in the atmosphere are deposited onto the surfaces in the absence of precipitation (Seinfeld and Pandis, 2006). Among the many N_r compounds, gaseous NH_3, HNO_3, NO_2, and aerosol NH_4^+, NO_3^-, and organic N are relatively high in the atmosphere. These compounds have vigorous chemical and biological activities and are relatively easily deposited (Galloway et al., 2004). Therefore, these compounds are usually considered the main parameters in quantifying dry N deposition (Xu et al., 2018; Yu et al., 2019; Chang et al., 2020). The factors that influence the dry deposition of gas-phase and particle-phase Nr species include atmospheric turbulence strength, the depositing species' chemical properties, and physicochemical properties (e.g., whether it is wet and the pH level) of the surface itself (Seinfeld and Pandis, 2006). The processes of dry deposition of gaseous and particulate N_r species generally have three steps as follows:

1. Aerodynamic transport down through the atmospheric surface layer to a skinny layer of stagnant air just adjacent to the surface.
2. Molecular (for gases) or Brownian (for particles) transport across this thin stagnant layer of air, called the *quasi-laminar sublayer*, to the surface itself.
3. Uptake at the surface.

Each of these steps contributes to the deposition velocity (V_d) (see detail in Sect.2.2.2) (Wesely, 2000). Dry deposition fluxes of N_r species can be measured by micrometeorological approaches or estimated by the inferential method, as depicted below.

2.2.1. Micrometeorological methods

Micrometeorological flux measurement methods include the aerodynamic gradient, eddy covariance, relaxed eddy accumulation, and time-averaged gradient (Fowler et al., 2001). These approaches are capable of producing averaged atmosphere-land exchange flux of the N_r species at a large area (>100 m^2) without the surrounding environment being perturbated (Sommar et al., 2013). Meanwhile, micrometeorological approaches also have limitations because they assume a uniform underlying surface, stationary turbulence, and adequate fetch (Fotiadi et al., 2005).

The aerodynamic gradient method applied to calculate the dry deposition (or emission) flux (F) of a specific N_r species is considered as the product of the turbulent diffusion coefficient (K) and the vertical air concentration gradient of the N_r species $\left(\frac{\partial c}{\partial z}\right)$ in the so-called constant flux layer (Dyer and Hicks, 2010), with the former mainly depended on the turbulent conditions (e.g., the friction velocity) and the latter depended on atmospheric concentrations of the target Nr species at two measuring heights. The parameterizations of K value and $\frac{\partial c}{\partial z}$ can be found in the study by Ke et al. (2020), who used the aerodynamic method and found that NO_x dry deposition flux above a subtropical forest in China was approximately 6.3 kg N ha^{-1} yr^{-1}. Also, the gradient method has been successfully applied for the measurements of land-atmosphere exchange fluxes of NH_3, HNO_3, and aerosol NH_4^+, and NO_3^- (Nemitz et al., 2004; Phillips et al., 2004; Neirynck et al., 2007; Wolff et al., 2010). For this method, an accurate determination of the concentration gradient is a demanding technical task since it is likely less than 5% of the mean concentration (Fowler et al., 2001). Besides, the gradient method has a disadvantage in making a correct interpretation of the measured fluxes when they are not conserved. This may happen because of the existence of reactions between gaseous and particulate Nr species (Wolff et al., 2010).

Above-canopy fluxes of the N_r species based on the eddy covariance method depend on the covariance between instantaneous deviations of wind speed and atmospheric concentrations themselves relative to an averaging period, and its calculation can be expressed as (Geddes and Murphy, 2014):

$$F = \frac{1}{n}\sum_{i=1}^{n}[(w_i - \overline{w})\cdot(c_i - \overline{c})] \quad (3)$$

where n is the number of data points per averaging period, w denotes vertical wind velocities, and c denotes the concerned N_r concentration (the subscript i denotes the instantaneous measurements, while the overbar represents the mean for the averaging period). Eddy covariance and the gradient methods require a precise (±10% precision) and fast-response sensor (e.g., 10 Hz) to measure the N_r (e.g., NO_2, NH_3, and HNO_3) concentrations and wind velocity (Fowler et al., 2001; Phillips et al., 2004). However, such sensors are not readily available, although a high-precision, fast response (10 Hz) open-path NH_3 sensor with an eddy covariance method has been demonstrated in the field measurement of NH_3 flux (Miller et al., 2014; Sun et al., 2015).

Compared with the eddy covariance method, the relaxed eddy accumulation method provides an approach for measuring single-height flux (Businger and Oncley, 1990), which are attractive for determining NH_3 fluxes over different ecosystems, such as grassland (Sutton et al., 2001) and cropland (Nelson et al., 2017; Lichiheb et al., 2019) because fast-response sensors are not required to measure NH_3 concentrations. The calculation formula is as follows:

$$F = \beta\sigma_w(\overline{c^{\uparrow}} - \overline{c^{\downarrow}}) \quad (4)$$

where $\overline{c^{\uparrow}} - \overline{c^{\downarrow}}$ is the difference in the mean concentrations of the N_r species (e.g., NH_3) between updrafts and downdrafts, σ_w denotes the standard deviations of vertical wind velocities, and β is an empirical constant (0.627) (Baker et al., 1992), but does varied with atmospheric stability (Fowler et al., 2001). The magnitude of the difference is typically as small as that associated with the aerodynamic gradient, but the eddy accumulation approach cannot require an estimate of eddy diffusivity. In the eddy accumulation method, the requirement for fast-response chemical sensors is replaced with the need for measurements of concentration differences between the upward and the downward moving eddies (Wesely and Hicks, 2000).

It must be recognized that a drawback to the three methods above is that the measurements are expensive and labor-intensive at large spatial and long-term scales. Therefore, the time-averaged gradient method was developed and employed for long-term N_r fluxes measurements at a relatively low cost. This method measures the averaged vertical N_r concentration gradient and the same meteorological factors as those considered in the gradient method. Despite cost-effectiveness, significant bias may also occur when the atmospheric condition is in high stability in which the vertical concentration gradients are increased because of very small diffusivity, causing an over-estimate of the realistic flux. To avoid this, a conditional time-averaged gradient method has been developed to measure the weekly or monthly mean flux of major N_r species (e.g., NH_3, HNO_3, and aerosol NH_4^+ and NO_3^-). Compared to the continuous sampling of the time-averaged gradient method, this method only measures the concentration gradient to exclude stable conditions from the measurement period (Famulari et al., 2010). Thus, the measurements cannot be performed in the circumstances of the low wind velocity, stable air, and inadequate fetch.

2.2.2. Inferential method

The use of micrometeorological approaches to measuring dry deposition generally needs fast-response sensors and uniform underlying surfaces, making establishing the site costly in terms of money and labor. Thus, it is hard to apply these methods at regional and national scales. Alternatively, the inferential method was proposed, which estimates the dry N_r deposition flux (F) as the product of the air concentrations at a specific height (C_Z) and itself dry deposition velocity (V_d):

$$F = -C_Z V_d \tag{5}$$

The V_d is not readily measured, which was normally calculated using a resistance analogy approach with empirical constants obtained from the literatures and measured on-site meteorological variables (Clarke et al., 1997; Zhang et al., 2001, 2003). For gaseous N_r species, the V_d is defined as the reciprocal of the sum of three resistances (Wesely and Hicks, 1977):

$$V_d = 1/(R_a + R_b + R_c) \tag{6}$$

in which R_a, R_b and R_c are the aerodynamic resistance (same value for all gases) between the measurement height and the surface, the *quasi laminar* boundary layer resistance (which only depend on the properties of gaseous N_r, e.g., molecular diffusivity in the air), and the canopy resistance for receptor itself, respectively. The schematic diagram of the model's pathways is shown in Fig. 2a.

R_a is parameterized as (Erisman et al., 1994):

$$R_a(z-d) = (ku_*)^{-1}\left[ln\left(\frac{z-d}{z0}\right) - \psi_h\left(\frac{z-d}{L}\right) + \psi_h\left(\frac{z0}{L}\right)\right] \tag{7}$$

where z is the measurement height of N_r species, k the von Karman constant (0.41), u_* the friction velocity, d the zero-plane displacement height, $z0$ the roughness length, ψ_h the integrated stability function for entrained scalars, and L the Monin−Obukhov length. d and $z0$ are usually taken as 0 m and 0.01 m, respectively, for bare soil (Shen et al., 2016) and 0.67 and 0.1 times the plant height, respectively, when the soils are covered with vegetations.

R_b is parameterized as (Hicks et al., 1987):

$$R_b = (2/ku_*)(S_c/P_r)^{2/3} \tag{8}$$

in which Sc/Pr denote the ratio of the Schmidt number to the Prandtl number.

R_c is calculated according to Wesely (1989) as

$$R_c = \left[\frac{1}{R_s + R_m} + \frac{1}{R_{cut}} + \frac{1}{R_{dc} + R_{cl}} + \frac{1}{R_{ac} + R_{gs}}\right]^{-1} \tag{9}$$

The brief introduction on all resistances in the Eq. (9) has been

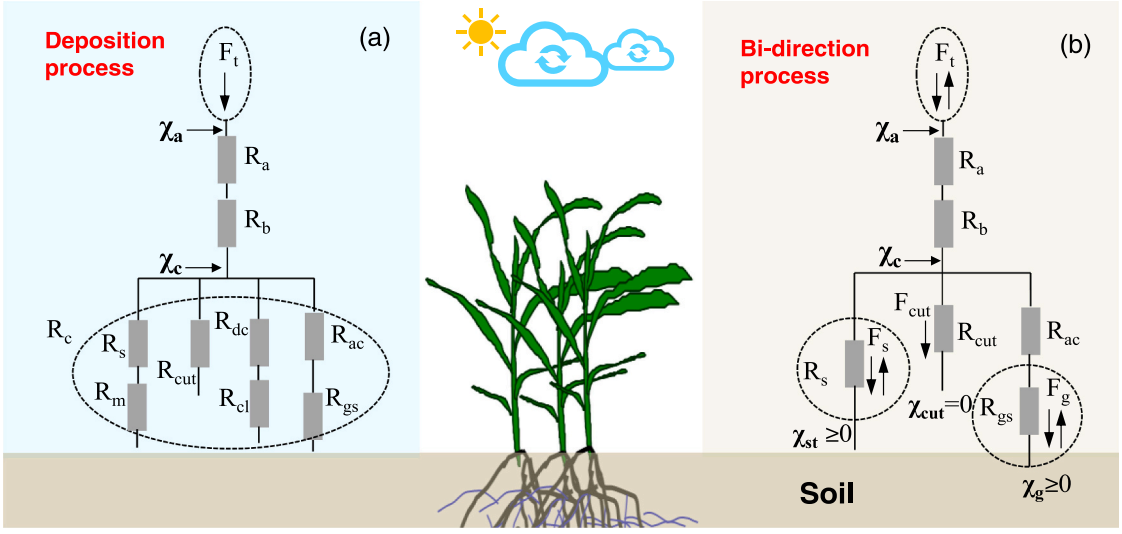

Fig. 2. Scheme of gaseous N_r dry deposition model (a) and the bi-directional NH_3 exchange model (b). F_t denotes overall flux at a reference height above the canopy, and F_s and F_g are bi-directional fluxes through stomata and above soil surface, respectively. x_a represents NH_3 concentration at the measurement height; x_c NH_3 concentration at the top of canopy; x_{st} and x_g are stomatal and soil NH_3 compensation points, respectively. Resistance terms contain R_a, the aerodynamic resistance; R_b, the quasi laminar boundary layer resistance; R_c, the overall canopy resistance; R_s, the stomatal resistance; R_m, the mesophyll resistance; R_{cut}, cuticular resistance; R_{dc}, the gas transmission resistance caused by the buoyant convection inside the canopy; R_{cl}, the resistance caused by the lower canopy leaves, branches, bark, or other exposed surfaces; R_{ac}, the aerodynamic resistance within the canopy; R_{gs}, the soil boundary layer resistance; and R_s, stomatal resistance.

provided in the caption of Fig. 2, and more details on parameterizations of them can be found in Wesely (1989).

For particulate N_r species, the commonly used parameterization of the dry deposition velocity is expressed as follows (Slinn, 1982):

$$V_d = \frac{1}{R_a + R_s} + V_g \tag{10}$$

where R_s is the surface resistance, and V_g is the gravitational settling velocity. Parameterizations of R_s and V_g have been provided in Zhang et al. (2001).

It is noteworthy that the land/atmosphere exchange of gaseous NH_3 is typically bi-directional over unfertilized as well as fertilized ecosystems (Sutton et al., 1998), and thus many bi-directional surface-atmosphere NH_3 exchange models with similarity in concept have been developed and employed in lots of applications (e.g., Flechard et al., 1999; Nemitz et al., 2000, 2001; Zhang et al., 2010). Wherein, the latest bi-directional exchange model developed by Zhang et al. (2010) is very similar to the two-layer model by Nemitz et al. (2001) with consideration of NH_3 exchange with leaf stomata and the soil surface. Besides, the model by Zhang et al. (2010) has been successfully applied in the air quality forecasting model to quantify the relative contributions of natural and anthropogenic sources on atmospheric NH_3 concentrations in the Athabasca Oil Sands region (Whaley et al., 2018). Here we summarized the bi-directional NH_3 exchange model by Zhang et al. (2010) for the readers' convenience. The schematic diagram of pathways in the model is depicted in Fig. 2b.

The NH_3 flux (F_t) above the canopy is parameterized as

$$F_t = -\frac{(x_a - x_c)}{(R_a + R_b)} \tag{11}$$

where x_a and x_c represent NH_3 concentrations at the measurement height and at the canopy top, respectively. x_c is calculated as

$$x_c = \left[\frac{x_a}{R_a + R_b} + \frac{x_{st}}{R_{st}} + \frac{x_g}{R_{ac} + R_{gs}}\right] \cdot \left[\frac{1}{R_a + R_b} + \frac{1}{R_{st}} + \frac{1}{R_{ac} + R_{gs}} + \frac{1}{R_{cut}}\right]^{-1} \tag{12}$$

If $x_a > x_c$, the flux will be downward, i.e., deposition process (negative value of F_t), while with $x_a < x_c$, the flux will be upward, i.e., emission process (positive value of F_t). Details on parameterizations of all resistances in Eq. (12) are provided in Zhang et al. (2010). Note that x_{st} and x_g in Eq. (12) are two crucial influencing parameters on the direction of the NH_3 flux, which is calculated based on the NH_4^+ concentration and pH in the leaf apoplast and soil (Zhang et al., 2010). Currently, detailed data on x_{st} and x_g of terrestrial ecosystems, especially for the major food cropping systems (e.g., maize and wheat), is very scarce, despite that some values of them have been summarized by Massad et al. (2010) for forests, some arable crops, short semi-natural (mostly heathlands) and grassland.

2.3. Other research methods for quantification of nitrogen deposition

2.3.1. Bioindicator method

Apart from the approaches for quantification of N wet and dry deposition mentioned earlier, atmospheric N_r deposition can also be measured through plants that play a vital role as primary receptors. It is commonly accepted that epiphytic lichens and mosses are useful bioindicators of atmospheric N deposition and have been adapted to determine N deposition fluxes at a regional scale worldwide, especially for areas where monitoring is currently sparse (Frati et al., 2007; Liu et al., 2008; Xiao et al., 2010, 2011; Qu et al., 2016). This is because lichens and mosses lack root systems and thus take up atmospheric N via their leaf surfaces, thereby resulting in their sensitivity to the N_r concentration in the atmosphere (Oishi, 2019). The reported relationships between N deposition and N contents in moss tissue are summarized in Table S1. Some moss species showed an excellent performance in quantifying atmospheric N deposition, such as *Pleurozium schreberi* (Brid.) Mitt., *Scleropodium purum* (Hedw.) Limpr. (Solga et al., 2005; Salemaa et al., 2008), epilithic *Haplocladium microphyllum* (Hedw.) (Liu et al., 2008), and a mixture of mosses (Xiao et al., 2010). Based on the linear equation between moss N concentration and N deposition, Xiao et al. (2010) reported that the total N deposition rates were 13.8–47.7 kg N ha^{-1} yr^{-1} at five sites in Yangtze River Basin, China. Schröder et al. (2014) found that the relationships between N concentrations in atmospheric deposition and mosses are country- and N compound-specific and coincide well with spatial patterns and temporal trends across Europe as a whole and in single European countries. However, occasionally N deposition fluxes and the moss N concentrations are weakly correlated (Stevens et al., 2011) or exhibited to be moss species-specific (Harmens et al., 2014), which may be resulted from the regulation of tissue loads in mosses because N plays a crucial role in the metabolism of organisms (Arroniz-Crespo et al., 2008). For accurate quantification of N deposition via mosses, the total N deposition fluxes (dry plus wet N deposition) containing dominant gaseous and particulate N_r species are recommended to establish the relationship between N deposition and moss N concentration, which is not sufficiently considered in all reported relationships listed in Table S1.

Nitrogen content and stable isotope composition in Liches were also used to monitor atmospheric N deposition passively and identify N pollution sources (Fenn et al., 2007; Root et al., 2015; Pinho et al., 2017; Hoffman et al., 2019). Comparatively high N content in lichens was found in areas close to pollution sources (Boltersdorf and Werner, 2014; Fenn et al., 2007; McMurray et al., 2013). However, the mechanisms by which lichens incorporate N could be influenced by N deposition fluxes and climate. The relationship between N content in lichens and N deposition could be more complicated rather than a simple linear relationship, partly because lichen N content is influenced by climatic variables such as the type and amount of precipitation and relative humidity (Root et al., 2013; McMurray et al., 2015). For example, based on the measurement at 84 study sites in western America, Root et al. (2013) found that estimated N deposition were moderately correlated ($R^2 = 0.58$) with lichen N concentration; and this relationship could be improved ($R^2 = 0.74$) with consideration of climate covariates including precipitation seasonality and temperature in the wettest quarter. Besides, total N deposition and speciation of N deposition also affect the relationship (Fremstad et al., 2005; Johansson et al., 2010; Munzi et al., 2019).

In addition to mosses and lichens, the vascular plant is often used as a bioindicator of the total N deposition. Determining N deposition with vascular plants was initially conducted with potted ryegrass (*Lolium perenne*), which is the so-called integrated total nitrogen input (ITNI) method (Sommer, 1988). Afterward, this technique was improved by adding ^{15}N as a tracer in the fertilizer (Mehlert et al., 1995), which is based on the dilution of this ^{15}N-tracer within a plant-liquid-sand system to determine total N input from the atmosphere. The ITNI method was previously applied in agroecosystems to quantify N input from the atmosphere into vegetables and cereal plants (He et al., 2007, 2010; Russow and Böhme, 2005; Weigel et al., 2000). More recently, this method was applied in peat bogs in Germany (Hurkuck et al., 2015) and a semiarid region of southern California (Sickman et al., 2019). Based on this method, the total N deposition was estimated at 80–100 kg N ha^{-1} yr^{-1} for a maize-wheat cropping system in the North China Plain, China (He et al., 2007, 2010), and 29.3 kg N ha^{-1} yr^{-1} in coastal sage scrub ecosystems in Riverside, California (Sickman et al., 2019). It has been found that plant biomass production has a strong influence on measured N deposition fluxes with the ITNI method (Sickman et al., 2019). When extrapolating deposition from modules to the landscape scale, measurements should be corrected for any significant difference in plant biomass between the individual ITNI modules and plant biomass. Due to biological variability, environmental interactions, and response delay of plants, standardization should be considered in biomonitoring to

achieve meaningful results. For example, using a single species as the receptor for N is usually limited by the species' geographic distribution. When plants are solely used as receptors for N, accurate quantification of total N deposition is limited. Detailed information on the monitoring process of N deposition by mosses and vascular plants has been provided elsewhere (Xiao et al., 2011; Sickman et al., 2019).

2.3.2. Satellite-based estimate

The technique of satellite remote sensing can be applied to estimate N dry and wet deposition. Currently, atmospheric remote sensing can detect the NH_3 and NO_2 in the atmosphere and has supplied continuous monitoring of daily NH_3 and NO_2 at the global scale, such as Infrared Atmospheric Sounding Interferometer for NH_3 (Van Damme et al., 2018) and Ozone Monitoring Instrument for NO_2 (Miyazaki et al., 2017). The concentration of NH_3 and NO_2 monitored by this technique refers to the total molecular content (molec.cm^{-2}) of the atmospheric column concentration from the ground to the tropopause (Liu et al., 2017a). The ground process mainly influences N deposition; therefore, it is necessary to convert the column concentration to the ground (Liu et al., 2017c). In general, dry deposition estimated by the satellite remote sensing is processed in two steps. First, the atmosphere chemical transition model is used to simulate the vertical concentration profiles of NH_3 and NO_2, and the satellite-observed column concentrations of NO_2 and NH_3 are converted to corresponding near-surface concentrations, respectively. Taking the MOZART-4 model as an example, MOZART-4 can output 56 verticals stratified concentrations of NO_2 and NH_3 from the ground upward. The profiles of NO_2 and NH_3 are obtained by simulating the concentration in each grid cell based on the Gaussian (Liu et al., 2017d, 2020b). There is currently no reliable satellite product for other inorganic nitrogen components in the atmosphere, such as HNO_3, aerosol NO_3^- and NH_4^+. The IASI product can simulate HNO_3 at a spatial resolution of $1^\circ \times 1^\circ$; however, this spatial resolution is relatively coarse, resulting in the inefficiency for estimating inorganic N deposition on a regional scale. Moreover, the IASI HNO_3 product is still in the development and verification stage, which has not been disclosed to the public and is currently not open access. The near-surface NH_3 and NO_2 concentration estimated based on the satellite remote sensing can be used to predict the near-surface concentrations of HNO_3 and aerosol NO_3^- and NH_4^+ (Liu et al., 2020a). After that, N_r concentration and V_d deduced from satellite data are used to calculate dry N deposition.

Inorganic N wet deposition estimated by the satellite remote sensing can be simplified to the product of the concentration of inorganic N in the atmosphere, precipitation, and erosion coefficient (Liu et al., 2017b). For the concentration of inorganic N_r in the atmosphere, remote sensing can be used to monitor NO_2 and NH_3; the precipitation can be obtained from the ground monitoring data or reanalysis data. However, for atmospheric inorganic N_r under precipitation events (including precipitation or snow), the simulation of the scavenging coefficient of inorganic N_r remains a major challenge and often contains considerable uncertainty. In order to improve the accuracy of the simulation by remote sensing, the relationship model (mixed utility model) between the monitoring of NO_2 and NH_3 by remote sensing, precipitation, and inorganic N wet deposition on the ground was constructed (Liu et al., 2017b, 2020a). Based on the NO_2 and NH_3 column concentration and precipitation in the monthly scale, the mixed utility model can be adapted to simulate wet N deposition. The mixed-utility model can be optimized by the NO_2 and NH_3 column concentrations and meteorological data from near-surface and satellite remote observations.

2.3.3. Model-based estimate

Many atmospheric chemistry transport models (ATMs), such as the Goddard Earth Observing System (GEOS) -Chem model (Xu et al., 2018a; Zhao et al., 2017), Community Multiscale Air Quality (CMAQ) model (Qiao et al., 2015), the Weather Research and Forecasting model coupled with Chemistry (WRF-Chem) model and the EMEP/MSC-W model (EMEP) (Chang et al., 2020), have been used to simulate N deposition. The simulation of wet N deposition is parameterized as in-cloud, below-cloud, and precipitation scavenging (Liu et al., 2001), while dry N deposition is calculated as the product of ambient concentrations of N_r species and V_d (which is the so-called inferential method as introduced in Sect. 2.2.2). Atmospheric N deposition flux simulated by ATMs usually requires emission inventories of NH_3 and NO_x calculated using top-to-down or bottom-to-up methods (Kang et al., 2016; Liu et al., 2016; Zhang et al., 2018). The accuracy of emission inventories directly affects the quantitative results of N deposition. However, the emission inventories of NH_3 and NO_x adopted to drive ATMs usually have large uncertainties; for example, estimates of China's NH_3 emissions differed by more than a factor of 2 (8.4–18.3 Tg yr^{-1}) in previous studies (Zhang et al., 2018). In part due to uncertainties in N_r emission inventories, the modeling conducted by Tan et al. (2018) showed that the modeling fluxes at 81–83% of the global stations were within 50% of the surface measurements; and an underestimation of the modeling wet deposition of NH_4^+ and NO_3^- occurred over Europe and East Asia, whereas the wet deposition of NO_3^- was overestimated over the eastern US. The ATMs can be configured with very high horizontal resolution (e.g., 1×1 km^2) on the regional scale (Kuik et al., 2016), and generally with relatively coarse on the global scale (Zhao et al., 2017), which cannot accurately reflect N_r deposition fluxes at local sites.

For NH_3, much effort has been made to develop a generalized parameterization for its bi-directional exchange to be incorporated into ATMs, such as AURAMS (A Unified Regional Air-quality Modeling System, developed by Environment Canada, Zhang et al., 2010) and CMAQ (Cooter and Bash, 2009). Unfortunately, most of the widely used ATMs (e.g., GEOS-Chem, EMEP) have not considered the bi-directional NH_3 schemes yet. A recent study by Whaley et al. (2018) incorporated the bidirectional flux parameterization (Zhang et al., 2010) into GEM-MACH (Global Environment Multiscale-Modeling Air quality and CHemistry) and simulated NH_3 flux over the Alberta and Saskatchewan region. Thus, most reported modeling on dry NH_3 deposition fluxes is still subjected to large uncertainties (Liu et al., 2017). Since the chemical reactions of dissolved organic N compounds are highly complicated, the mode description of their generation and scavenging mechanisms is limited. Therefore, it is not easy to use the ATMs to simulate the wet deposition process of dissolved organic N accurately.

3. Nitrogen deposition monitoring networks

3.1. Global monitoring networks and the resulting wet nitrogen deposition flux

The NADP (US National Atmospheric Deposition Program), EMEP (Co-operative Programme for Monitoring and Evaluation of the Long Range Transmissions of Air Pollutants in Europe), and EANET (Acid Deposition Monitoring Network in East Asia) are three well-known networks (Fig. 3), which take the leads of N deposition monitoring in the United States, Europe, and East Asia, respectively. The NADP was established in 1978 and now has 263 sites. This network aims to provide a basis for researching the spatial characteristics and temporal variations of atmospheric deposition (e.g., sulfur, nitrogen, and mercury) in the United States. The EMEP network was initiated in the early 1970s, aiming to solve transboundary air pollution by providing standardized air environmental quality data and providing governments and parties with a scientific basis for air pollution control. Currently, 269 monitoring sites are included to monitor the particulate matter and associated carbonaceous and inorganic compounds, ozone, heavy metals, persistent organic pollutants, and volatile organic compounds. The EANET started in 1998. There are 54 sites established in 13 East Asia countries for monitoring acid deposition, dry, and wet N deposition. This network is essential to reach a consensus on the state of acid deposition in East Asia and provides scientific suggestions for decision-makers at all levels to reduce environmental pollution, such as acidification. For quantification of N deposition, the common point of these three networks is that

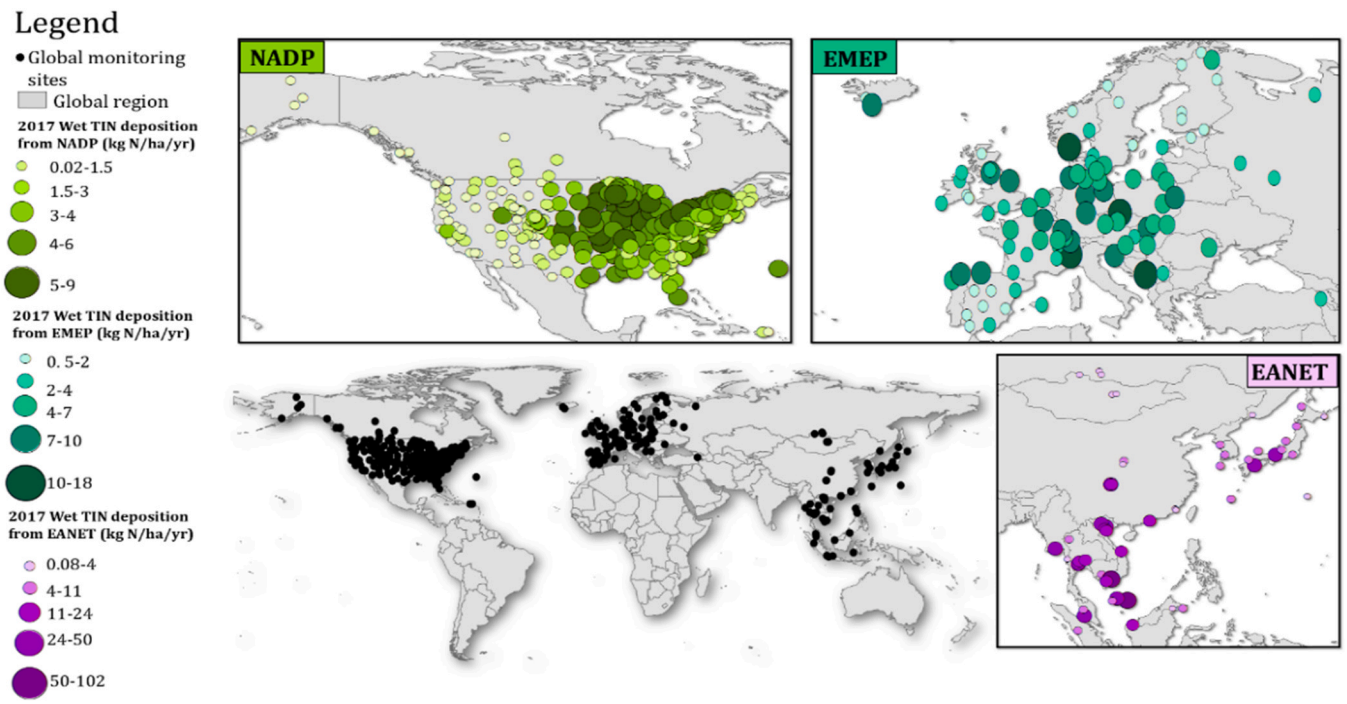

Fig. 3. The total wet inorganic nitrogen deposition fluxes measured at 266 sites in NADP (US National Atmospheric Deposition Program, http://nadp.slh.wisc.edu/NADP/networks.aspx), 90 sites in EMEP (Co-operative Programme for Monitoring and Evaluation of the Long Range Transmissions of Air Pollutants in Europe, https://projects.nilu.no//ccc/reports.html), and 57 sites in EANET (Acid Deposition Monitoring Network in East Asia, https://www.eanet.asia/event-and-activities/) in 2017 (NH_4^+ and NO_3^- concentrations in precipitation, and precipitation amount at sites in each network were collected from the corresponding websites listed above. The calculated wet N deposition flux (which is a product of the concentrations and precipitation amount for all sites are provided in the Supplement Material).

they mainly focus on wet deposition measurements of NH_4^+ and NO_3^- and consider gaseous and particulate N_r concentrations.

The above three deposition networks are widely used for quantifying regional N deposition fluxes (e.g., Tørseth et al., 2012, Ban et al., 2016; Li et al., 2016; Tan et al., 2020). However, most of the above studies were carried out in different countries in different periods, resulting in the difficulty to accurately evaluate the N_r pollution and the magnitude of N deposition at a global scale. Given this, we calculated the total wet inorganic nitrogen (TIN (total inorganic nitrogen), NH_4^+-N plus NO_3^--N) deposition from the three networks in 2017 as an example to analyze the spatial pattern of the global wet TIN deposition. As shown in Fig. 3, in 2017, annual wet N deposition in the United States (266 sites) averaged 3.2 ± 1.8 kg N ha^{-1} yr^{-1}, which was relatively lower compared to 4.8 ± 3.1 kg N ha^{-1} yr^{-1} in Europe (90 sites) and 15.6 ± 19.3 kg N ha^{-1} yr^{-1} in East Asia (57 sites). The Low wet N deposition (0.02–1.5 kg N ha^{-1} yr^{-1}) was mainly concentrated in the western part of the United States, whereas the hotspot region with high wet N deposition (4–9 kg N ha^{-1} yr^{-1}) is in the northeast part of the United States and the Great Lakes. Some parts of Indonesia, Vietnam, China, Japan, Thailand, and Malaysia are hotspots of wet N deposition (24–102 kg N ha^{-1} yr^{-1}) in East Asia. Considering limited EANET sites in China, the magnitude and spatio-temporal N deposition pattern in China will be summarized in Section 3.2 based on the results from other networks. Europe shows the lowest N deposition, compared to America and Asia. In Europe, Italy, Norway, Poland, Montenegro, and Belarus show relatively high levels of wet N deposition (10–18 kg N ha^{-1} yr^{-1}), while countries with low deposition levels (0.5–2 kg N ha^{-1} yr^{-1}) are Iceland, Finland, Sweden, Spain, UK, Ireland, Latvia, Norway, and Sweden.

Direct measurements of dry deposition are difficult to make in monitoring networks because of the requirements for highly sophisticated methods and instrumentation. The few monitoring networks also employed the inferential method to estimate dry deposition, i.e., the Canadian Air and Precipitation Network (CAPMoN, http://www.ec.gc.ca/rs-mn/default.asp?lang=En&n%20=752CE271–1), the Clean Air Status and Trends Network (CASTNET, http://java.epa.gov/castnet/), and EANET.

3.2. Nitrogen deposition monitoring networks in China and resulting spatiotemporal pattern of N deposition

China has been one of the global hotspots of N deposition due to the dramatically increasing anthropogenic N_r emissions (Wen et al., 2020). Currently, China has two major N deposition monitoring networks: the Nationwide Nitrogen Deposition Monitoring Network (NNDMN) operated by China Agricultural University (Xu et al., 2015, 2019), and the Center of Ecosystem Research Network (CERN) operated by the Chinese Academy of Sciences (Zhu et al., 2015). The NNDMN considers simultaneous dry and wet/bulk N deposition of major N_r species in the air (NH_3, NO_2, HNO_3, aerosol NH_4^+ and NO_3^-), and precipitation (NH_4^+ and NO_3^-). In contrast, the CERN measures wet-only N deposition of inorganic and organic N_r species. The dry N deposition estimated by the NNMDN was based on the inference method. As shown in Fig. 4, the total N deposition (wet/bulk plus dry N deposition) measured in China was 39.9 kg N ha^{-1} yr^{-1} averaged from the measurements at 43 NNDMN sites. Total N deposition of 43 sites was ranked by land use as urban > rural > background sites (Xu et al., 2015). Except for significantly higher values in northern rural sites, annual dry N deposition fluxes were comparable at urban and background sites in northern and southern regions (Xu et al., 2018). More recently, based on measurements from 66 new NNDMN sites, Wen et al. (2020) also reported similar findings to those from Xu et al., (2015, 2018), and meanwhile demonstrated that the total N deposition exhibited a downward trend in 2011−2018 in China, confirming the effectiveness of the current air clean actions (B. Zheng et al., 2018; X.D. Zheng et al., 2018). The NNDMN monitored bulk N deposition, and thus the results should be somewhat higher than actual wet-only N deposition, as mentioned in Sect. 2.1. Additionally, quantification of organic N deposition is currently not a focus in the NNDMN, although relevant measurements were conducted before 2010

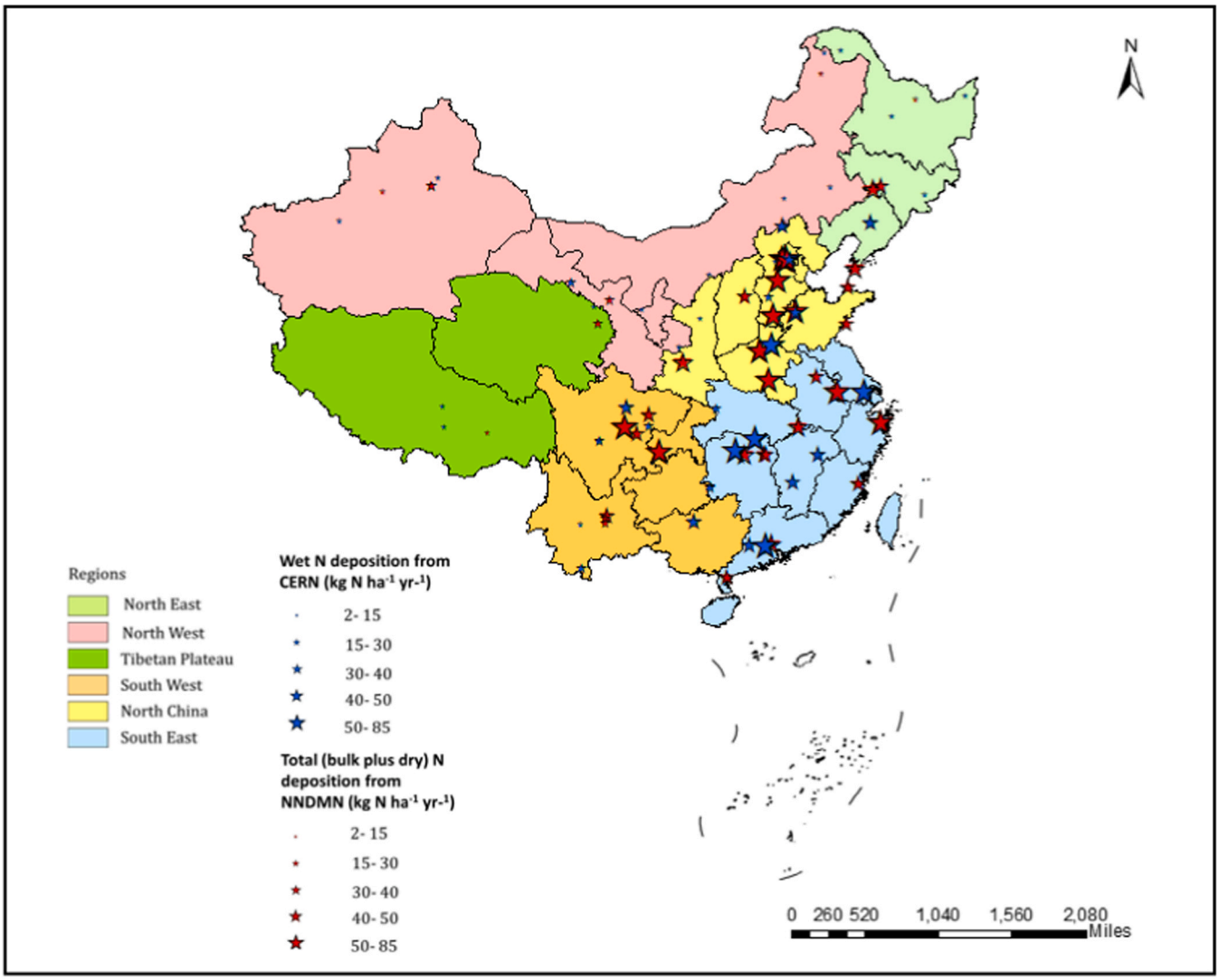

Fig. 4. Wet N deposition from the Center of Ecosystem Research Network (CERN, 41 sites) and total (dry plus bulk deposition) N deposition from Nationwide Nitrogen Deposition Monitoring Network (NNDMN, 43 sites) in China (data shown were collected from Zhu et al. (2015) and Xu et al. (2015) and are also provided in the Supplement Material).

(Zhang et al., 2012). In this regard, the CERN can provide details on wet-only N deposition fluxes of inorganic and organic N_r in China. Across 41 CERN sites, the total wet N deposition was 18.02 kg N ha^{-1} yr^{-1}, while the highest wet N deposition for Southwest and east China were more than 35 kg N ha^{-1} yr^{-1}. The lowest wet N deposition for northwest China, especially in Inner Mongolia and Xinjiang provinces, was approximately 2.5 kg N ha^{-1} yr^{-1}. Compared to other countries, annual mean wet N deposition (NH_4^+-N and NO_3^--N) fluxes in China (15.8 ± 11.1 kg N ha^{-1} yr^{-1}) was 3–5 times higher than that in the United States and Europe, but was close to that in East Asia (Figs. 3 and 4). Although NADP, EANET, EMEP, NNDMN, and CERN play a pivotal role in quantification of global N deposition, large areas of corresponding countries (e.g., western parts of China and the United States) and islands do not have adequate and evenly distributed monitoring sites, which may lead to losing hotspots of N deposition. Organic nitrogen deposition is a crucial part of the global N cycle (Neff et al., 2002), but currently is not measured in NADP, EANET, EMEP, and NNDMN. Dissolved organic nitrogen (DON) accounted for approximately 25% of the total dissolved N in global wet deposition (Jickells et al., 2013) and about 25% of China's bulk N deposition (Zhang et al., 2012). According to a meta-analysis by Jiang et al. (2013), the DON deposition in China was substantially higher than that of the world. For DON measurements, the quality control systems performed during the entire sampling, storage, and analysis are of great importance. Any improper storage process or delayed measurements may underestimate DON deposition (Cornell et al., 2003; Jickells et al., 2013).

Besides, regional-scale modeling tools and satellite observations were also used to explore the spatial pattern of N deposition in China (Zhao et al., 2017; Yu et al., 2019). For example, based on a remote sensing model and the published dataset, Yu et al. (2019) deeply elucidated the spatial characteristics of N deposition in China: (1) wet deposition fluxes of reduced (NH_x) and oxidized (NO_y) N were the highest in North, East and Central China; whereas dry deposition fluxes of them both reach the maximum in North China; (2) the spatial pattern of the total N deposition (20.4 ± 2.6 kg N ha^{-1} yr^{-1}) is similar to those of NH_x and NO_y deposition (Fig. 5). They also found that fossil fuel-based NO_x emissions and agricultural NH_3 emission collectively accounted for 62–99% of the spatiotemporal trend of total N deposition in China (Yu et al., 2019). The total N deposition rates differed slightly amongst the above studies, but it is commonly agreed that the dry N deposition and wet N deposition made almost equal contributions to the total N deposition at the national scale (Xu et al., 2015; Zhao et al., 2017; Yu et al., 2019).

For the annual variation of N deposition, significant progress has

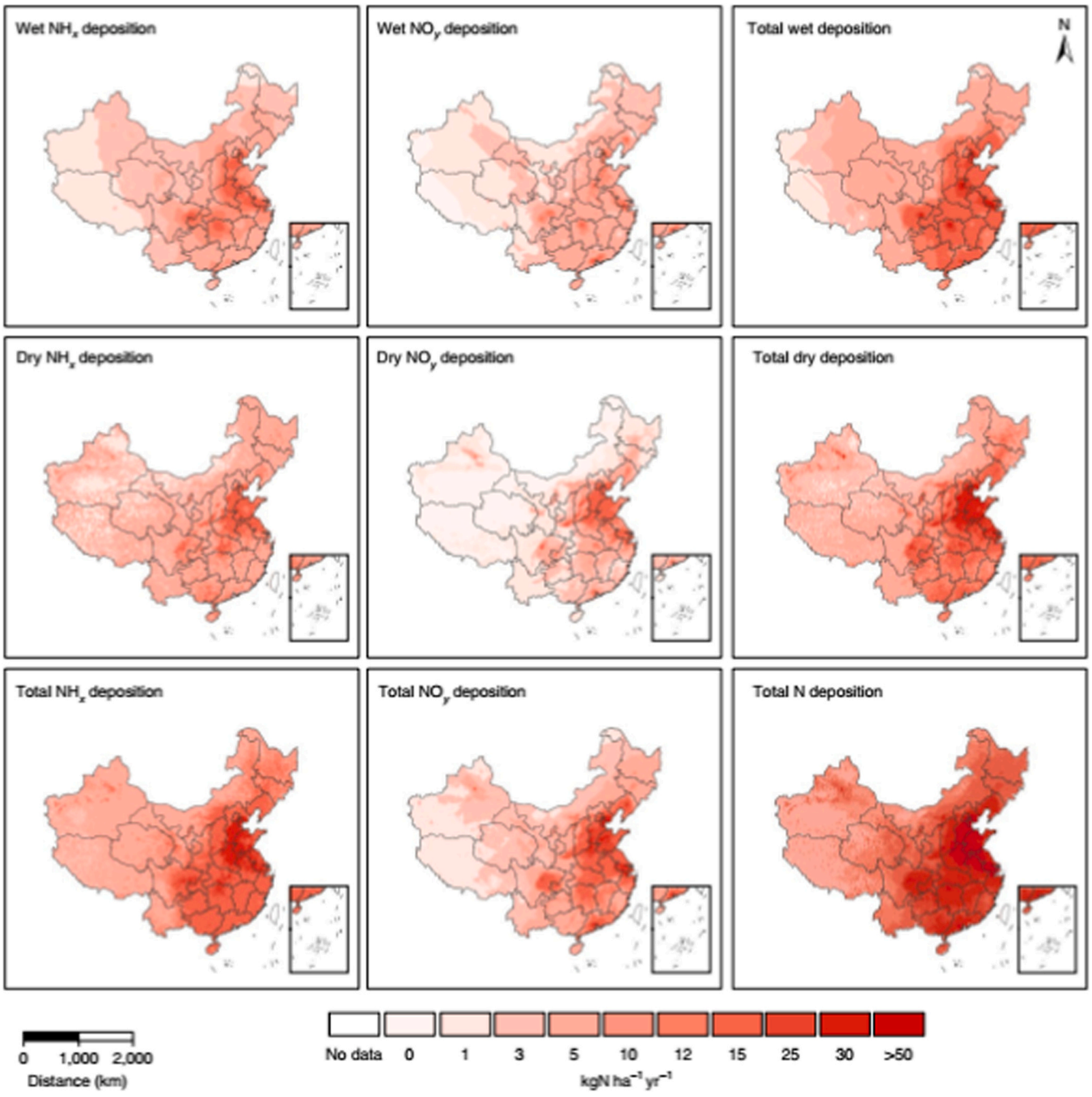

Fig. 5. Spatial patterns of atmospheric N deposition over China in 2011–2015 (cited from Yu et al. (2019)).

been achieved in many studies (Yu et al., 2019; Wen et al., 2020). For instance, Liu et al. (2013) synthesized historical data on bulk N deposition in China and found that its fluxes significantly increased between the 1980s (13.2 kg N ha^{-1} yr^{-1}) and the 2000s (21.1 kg N ha^{-1} yr^{-1}). Yu et al. (2019) further demonstrated that the total N deposition in China has shifted from an upward trend to stability in 1980–2015, in which wet N deposition fluxes peaked in 2001–2005 whereas a continuous increase in dry N deposition. More recently, Wen et al. (2020) further reported a whole story of N deposition across China over the last four decades, and they found that bulk and dry N deposition exhibited a downward trend in 2011–2018, mainly attributable to the decreasing oxidized N deposition.

Although the spatiotemporal trend of N deposition in China has been well studied, some pivotal issues need to be solved to improve the accuracy of the results. For example, some uncertainties may exist in the reported NH_3 deposition fluxes due to the following two causes: (1) lack of reliable data of emission factors for modeling at the level of local activities that limit the temporal and geographical distribution of atmospheric NH_3 concentration in the modeling processes; (2) bidirectional NH_3 exchange scheme is not incorporated within the atmospheric transport models (as mentioned in Sect. 2.3.3) and satellite-based method, which may overestimate dry NH_3 deposition, particularly in agricultural regions.

As introduced in detail in this study, each method of estimating N deposition has advantages and limitations, and its applicability depends on spatial and temporal scales. Here we proposed a comprehensive framework for quantification of wet and dry deposition of dominant N_r species at the single site and regional or national scale (Fig. 6). The

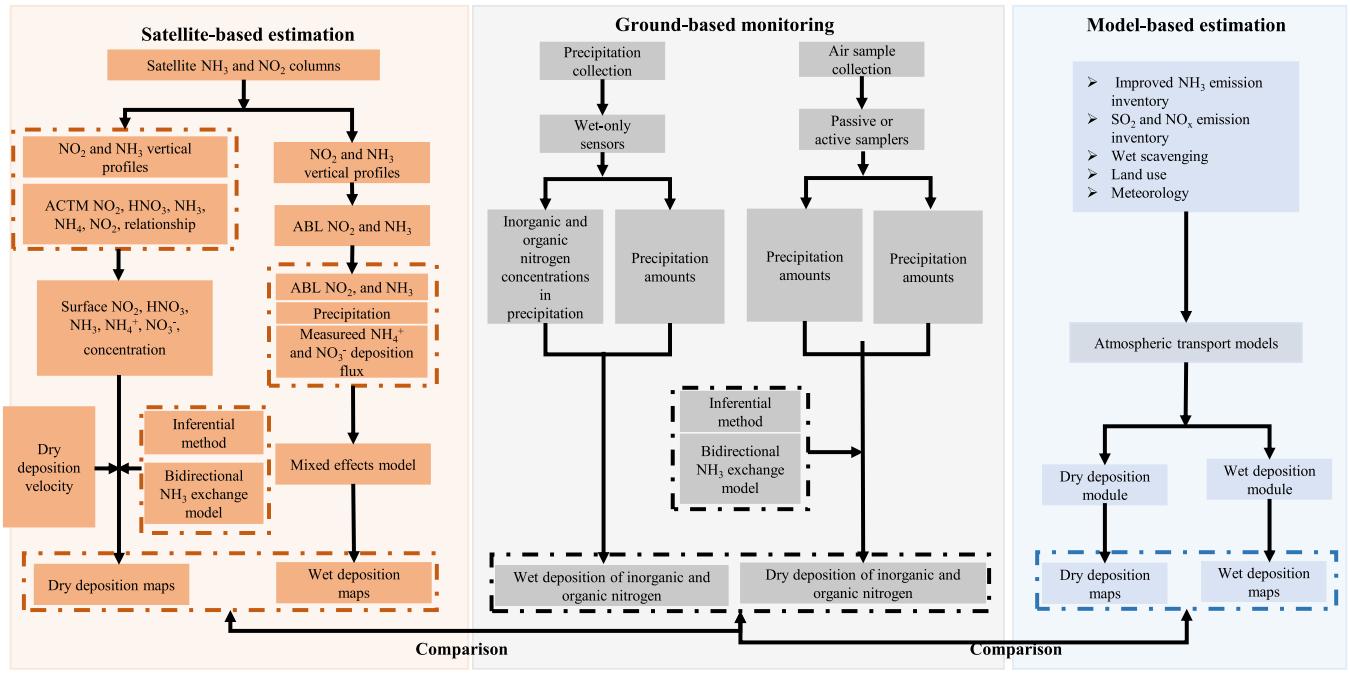

Fig. 6. A proposed framework to quantify dry and wet deposition of reactive nitrogen (ACTM and ABL means atmospheric chemistry transport model and atmospheric boundary layer, respectively).

framework consists of three sub-frameworks for ground-based monitoring, atmospheric chemical transport modeling (ACTM), and satellite-based estimation. For ground-based monitoring at a single site, we recommend using wet-only sensors for wet deposition measurements of inorganic and organic N_r species (Kuang et al., 2016), and considering dominant N_r species in the air (gaseous NH_3, HNO_3, NO_2, and particulate NH_4^+, NO_3^-, and organic N) in the quantification of dry deposition using passive samplers and active samplers (e.g., DEnuder for Long-Term Atmospheric sampling, Tang et al., 2009). The inferential method can be used to calculate dry deposition of dominant N_r species except for NH_3, of which the dry deposition flux should be quantified using the bi-directional exchange model (Zhang et al., 2010). For quantification of N deposition at a regional or national scale, improved satellite-based and model-based methods are recommended. For the application of satellite observations, the improvements fall into three categories (Liu et al., 2020b; Liu and Du, 2020): (1) improving the spatial and temporal resolution of satellite-derived products and using new data retrieval methods to optimize the data products; (2) applying satellite-derived near-surface N_r concentrations to estimate dry N deposition flux and the NO_2 and NH_3 column within the atmospheric boundary layer for estimating wet N deposition; (3) using bi-directional NH_3 exchange model to calculate dry NH_3 deposition flux. For modeling method, we recommend improving necessary inputs (e.g., NH_3 and NO_x emission inventories), the dry module (e.g., considering bi-directional NH_3 exchange scheme), and the wet module (reducing the uncertainty of the scavenging coefficient) to improve the accuracy of estimation. To accurately quantify N deposition fluxes, it is indispensable to use a combined method of monitoring, modeling, and remote sensing with comparisons conducted with each other.

4. Summary and outlook

Uncertainties exist in monitoring or modeling the wet and dry N deposition at the field, regional, and national scales. For dry deposition, micrometeorological approaches can provide direct N_r flux (deposition or emission) measurements and have been used extensively at the field scale. However, it is not easy to apply them at a regional scale due to labor-intensive and the need for expensive instruments and the limitation of field conditions. Alternatively, the inferential method is a useful avenue to quantify dry N deposition at a broad scale. Routine measurement-based inferential estimates of dry deposition are made in CAPMoN and CASTNET in North America, EANET in East Asia and NNDMN in China. Some uncertainties exist in NH_3 dry deposition quantification due to missing consideration of bi-directional NH_3 exchange in the surface-atmosphere. Wet/bulk N deposition measurements are included in most monitoring networks such as NADP (by wet-only sampling), EANET (by wet-only sampling), EMEP (by wet-only sampling or a bulk collector in different countries), NNDMN (by a bulk collector) and CERN (by wet-only sampling). For wet deposition, the uncertainty is mainly sourced from different concepts, sampling procedures, and analysis approaches adopted in existing monitoring networks, making the comparability of data compromised. The wet inorganic N deposition in China was higher than that in the United States, European countries, and other East Asia countries. Organic N deposition quantification usually is not included in most monitoring networks (e.g., NADP, EANET, EMEP, NNDMN). Both wet and dry N deposition fluxes should be considered for establishing the relationship between the N deposition and N concentration in moss tissue when using moss species as an indicator; in contrast, the ITNI method should be validated with the additional methods (e.g., the inferential method) to reduce its uncertainties. For satellite sensing, some uncertainties also exist in the transformation of tropospheric column concentrations of NH_3 and NO_2 into surface N_r concentrations in the estimate of dry N deposition and scavenging coefficient in wet N deposition. These uncertainties may limit our understanding of the wet and dry deposition processes and their potential eco-environmental impacts.

Therefore, we suggest future work to focus on the following aspects: (1) establishing a network in combination with monitoring stations with consideration of major N_r in the dry and wet N deposition, especially including the organic nitrogen; (2) optimizing the spatial location of the monitoring network and establishing more representative sites in areas for which limited data are available; (3) selecting unified sampling, storage, and analysis methods; (4) completing biomonitoring and satellite observation networks of ambient N_r concentrations and deposition; (5) reducing uncertainties in N_r deposition fluxes, especially the simulation of the NH_3 dry deposition rate, through an in-depth

understanding of the bi-directional NH_3 exchange process; and (6) enhancing international cooperation concerning the nitrogen deposition measurement, modeling, and environmental impact assessment.

CRediT authorship contribution statement

Qi Zhang, Yanan Li, Wen Xu: Designed the study. **Qi Zhang, Yanan Li, Wen Xu:** Prepared the figures and tables, Wrote the original draft. All the co-authors contributed to the revision of the manuscript.

Declaration of Competing Interest

The authors declare that they have no known competing financial interests or personal relationships that could have appeared to influence the work reported in this paper.

Acknowledgments

This work was supported by China Scholarship Council (No. 201913043), Key Consulting Project of the Chinese Academy of Engineering (2019-XZ-25), Key Consulting Project of the Chinese Academy of Engineering (2019-XZ-69), and Beijing Advanced Discipline.

Appendix A. Supporting information

Supplementary data associated with this article can be found in the online version at doi:10.1016/j.ecoenv.2021.112180.

References

Abdolahnejad, A., Jafari, N., Mohammadi, A., Miri, M., Hajizadeh, Y., 2018. Mortality and morbidity due to exposure to ambient NO_2, SO_2, and O_3 in Isfahan in 2013–2014. Int. J. Prev. Med. 9, 11. https://doi.org/10.4103/ijpvm.IJPVM_387_16.

Arroniz-Crespo, M., Leake, J.R., Horton, P., Phoenix, G.K., 2008. Bryophyte physiological responses to, and recovery from, long-term nitrogen deposition and phosphorus fertilisation in acidic grassland. New Phytol. 180, 864–874. https://doi.org/10.1111/j.1469-8137.2008.02617.x.

Baker, J.M., Norman, J.M., Bland, W.L., 1992. Field-scale application of flux measurement by conditional sampling. Agr. Meteorol. 62, 31–52. https://doi.org/10.1016/0168-1923(92)90004-N.

Ban, S., Matsuda, K., Sato, K., Ohizumi, T., 2016. Long-term assessment of nitrogen deposition at remote EANET sites in Japan. Atmos. Environ. 146, 70–78. https://doi.org/10.1016/j.atmosenv.2016.04.015.

Boltersdorf, S.H., Werner, W., 2014. Lichens as a useful mapping tool? An approach to assess atmospheric N loads in Germany by total N content and stable isotope signature. Environ. Monit. Assess. 186, 4767–4778. https://doi.org/10.1007/s10661-014-3736-3.

Businger, J., Oncley, S.P., 1990. Flux measurement and conditional sampling. J. Atmos. Ocean Technol. 7, 349–352. https://doi.org/10.1175/1520-0426(1990)007<0349:fmwcs>2.0.co;2.

Chang, M., Cao, J.C., Ma, M.R., Liu, Y.M., Liu, Y.Q., Chen, W.H., Fan, Q., Liao, W.H., Jia, S.G., Wang, X.M., 2020. Dry deposition of reactive nitrogen to different ecosystems across eastern China: a comparison of three community models. Sci. Total Environ. 720, 137548 https://doi.org/10.1016/j.scitotenv.2020.137548.

Clarke, J.F., Edgerton, E.S., Martin, B.E., 1997. Dry deposition calculations for the Clean Air Status and Trends Network. Atmos. Environ. 31, 3667–3678. https://doi.org/10.1016/S1352-2310(97)00141-6.

Cooter, E.J., Bash, J.O., 2009, A process based ammonia emission model for agricultural soils. NADP Annual meeting and scientific symposium, October 8.

Cornell, S.E., Jickells, T.D., Cape, J.N., Rowland, A.P., Duce, R.A., 2003. Organic nitrogen deposition on land and coastal environments: a review of methods and data. Atmos. Environ. 37, 2173–2191. https://doi.org/10.1016/S1352-2310(03)00133-X.

Van Damme, M., Clarisse, L., Whitburn, S., Hadji-Lazaro, J., Hurtmans, D., Clerbaux, C., Coheur, P.F., 2018. Industrial and agricultural ammonia point sources exposed. Nature 564, 99–103. https://doi.org/10.1038/s41586-018-0747-1.

Dämmgen, U., Erisman, J.W., Cape, J.N., Grünhage, L., Fowler, D., 2005. Practical considerations for addressing uncertainties in monitoring bulk deposition. Environ. Pollut. 134, 535–548. https://doi.org/10.1016/j.envpol.2004.08.013.

Dyer, A.J., Hicks, B.B., 2010. Flux-gradient relationships in the constant flux layer. Q. J. R. Meteorol. Soc. 96 (410), 715–721. https://doi.org/10.1002/qj.49709641012.

Erisman, J.W., Vanpul, A., Wyers, P., 1994. Parametrization of surface-resistance for the quantification of atmospheric deposition of acidifying pollutants and ozone. Atmos. Environ. 133, 403–413. https://doi.org/10.1016/1352-2310(94)90433-2.

Famulari, D., Fowler, D., Nemitz, E., Hargreaves, K.J., Storeton-West, R.L., Rutherford, G., Tang, Y.S., Sutton, M.A., Weston, K.J., 2010. Development of a low-cost system for measuring conditional time-averaged gradients of SO_2 and NH_3. Environ. Monit. Asses. 161, 11–27.

Fattore, F., Bertolini, T., Materia, S., Gualdi, S., Thongo M'Bou, A., Nicolini, G., Valentini, R., De Grandcourt, A., Tedesco, D., Castaldi, S., 2014. Seasonal trends of dry and bulk concentration of nitrogen compounds over a rain forest in Ghana. Biogeosciences 11, 3069–3081. https://doi.org/10.5194/bg-11-3069-2014.

Fenn, M.E., Geiser, L., Bachman, R., Blubaugh, T.J., Bytnerowicz, A., 2007. Atmospheric deposition inputs and effects on lichen chemistry and indicator species in the Columbia River Gorge, USA. Environ. Pollut. 146, 77–91. https://doi.org/10.1016/j.envpol.2006.06.024.

Fenn, M.E., Poth, M.A., 2004. Monitoring nitrogen deposition in throughfall using ion exchange resin columns: a field test in the San Bernardino Mountains. J. Environ. Qual. 33, 2007–2014. https://doi.org/10.2134/jeq2004.2007.

Fenn, M.E., Sickman, J.O., Bytnerowicz, A., Clow, D.W., Molotch, N.P., Pleim, J.E., Tonnesen, G.S., Weathers, K.C., Padgett, P.E., Campbell, D.H., 2009. Methods for measuring atmospheric nitrogen deposition inputs in arid and montane ecosystems of western North America. Dev. Environ. Sci. 9, 179–228.

Flechard, C.R., Fowler, D., Sutton, M.A., Cape, J.N., 1999. A dynamic chemical model of bi-directional ammonia exchange between semi-natural vegetation and the atmosphere. Q. J. Roy. Meteor. Soc. 125, 2611–2641. https://doi.org/10.1002/qj.49712555914.

Fotiadi, A.K., Lohou, F., Druilhet, A., Serça, D., Said, F., Laville, P., Brut, A., 2005. Methodological development of the conditional sampling method. Part II: quality control criteria of relaxed eddy accumulation flux measurements. Bound-Lay. Meteorol. 117, 577–603. https://doi.org/10.1007/s10546-005-4497-x.

Fowler, D., Coyle, M., Flechard, C., Hargreaves, K., Nemitz, E., Storeton-West, R., Sutton, M., Erisman, J.W., 2001. Advances in micrometeorological methods for the measurement and interpretation of gas and particle nitrogen fluxes. Plant Soil 228, 117–129.

Fowler, D., Steadman, C.E., Stevenson, D., Coyle, M., Rees, R.M., Skiba, U.M., Sutton, M. A., Cape, J.N., Dore, A.J., Vieno, M., Simpson, D., Zaehle, S., Stocker, B.D., Rinaldi, M., Facchini, M.C., Flechard, C.R., Nemitz, E., Twigg, M., Erisman, J.W., Butterbach-Bahl, K., Galloway, J.N., 2015. Effects of global change during the 21st century on the nitrogen cycle. Atmos. Chem. Phys. 15, 13849–13893. https://doi.org/10.5194/acp-15-13849-2015.

Frati, L., Santoni, S., Nicolardi, V., Gaggi, C., Brunialti, G., Guttova, A., Gaudino, S., Pati, A., Pirintsos, S.A., Loppi, S., 2007. Lichen biomonitoring of ammonia emission and nitrogen deposition around a pig stockfarm. Environ. Pollut. 146, 311–316. https://doi.org/10.1016/j.envpol.2006.03.029.

Fremstad, E., Paal, J., Möls, T., 2005. Impacts of increased nitrogen supply on norwegianlichen-rich alpine communities: a 10-year experiment. J. Ecol. 93, 471–481. https://doi.org/10.1111/j.1365-2745.2005.00995.x.

Galloway, J.N., Dentener, F.J., Capone, D.G., Boyer, E.W., Howarth, R.W., Seitzinger, S. P., Asner, G.P., Cleveland, C.C., Green, P.A., Holland, E.A., Karl, D.M., Michaels, A. F., Porter, J.H., Townsend, A.R., Vorosmarty, C.J., 2004. Nitrogen cycles: past, present, and future. Biogeochemistry 70, 153–226. https://doi.org/10.1007/s10533-004-0370-0.

Geddes, J.A., Murphy, J.G., 2014. Observations of reactive nitrogen oxide fluxes by eddy covariance above two midlatitude North American mixed hardwood forests. Atmos. Chem. Phys. 14, 2939–2957. https://doi.org/10.5194/acp-14-2939-2014.

Gilliam, F.S., Burns, D.A., Driscoll, C.T., Frey, S.D., Lovett, G.M., Watmough, S.A., 2019. Decreased atmospheric nitrogen deposition in eastern North America: predicted responses of forest ecosystems. Environ. Pollut. 244, 560–574. https://doi.org/10.1016/j.envpol.2018.09.135.

Goncalves, F.L.T., Andrade, M.F., Forti, M.C., Astolfo, R., Ramos, M.A., Massambani, O., Melfi, A.J., 2003. Preliminary estimation of the rainfall chemical composition evaluated through the scavenging modelingfor north-eastern Amazonian region (Amapa State, Brazil). Environ. Pollut. 121, 63–73. https://doi.org/10.1016/S0269-7491(02)00209-9.

Harmens, H., Schnyder, E., Thöni, L., Cooper, D.M., Mills, G., Leblond, S., Mohr, K., Poikolainen, J., Santamaria, J., Skudnik, M., Zechmeister, H.G., Lindroos, A.J., Hanus-Illnar, A., 2014. Relationship between site-specific nitrogen concentrations in mosses and measured wet bulk atmospheric nitrogen deposition across Europe. Environ. Pollut. 194, 50–59. https://doi.org/10.1016/j.envpol.2014.07.016.

He, C.E., Liu, X., Fangmeier, A., Zhang, F., 2007. Quantifying the total airborne nitrogen input into agroecosystems in the North China Plain. Sci. Dir. 121, 395–400. https://doi.org/10.1016/j.agee.2006.12.016.

He, C.E., Wang, X., Liu, X.J., Fangmeier, A., Christie, P., Zhang, F.S., 2010. Nitrogen deposition and its contribution to nutrient inputs to intensively managed agricultural ecosystems. Ecol. Appl. 20, 80–90. https://doi.org/10.1890/08-0582.1.

Hicks, B.B., Baldocchi, D.D., Meyers, T.P., Hosker Jr., R.P., Matt, D.R., 1987. A preliminary multiple resistance routine for deriving dry deposition velocities from measured quantities. Water Air Soil Pollut. 36, 311–330. https://doi.org/10.1007/BF00229675.

Hoffman, A.S., Albeke, S.E., McMurray, J.A., David Evan, R., Williams, D.G., 2019. Nitrogen deposition sources and patterns in the Greater Yellowstone Ecosystem determined from ion exchange resin collectors, lichens, and isotopes. Sci. Total Environ. 683, 709–718. https://doi.org/10.1016/j.scitotenv.2019.05.323.

Hurkuck, M., Brümmer, C., Mohr, K., Spott, O., Well, R., Flessa, H., Kutsch, W.L., 2015. Effects of grass species and grass growth on atmospheric nitrogen deposition to a bog ecosystem surrounded by intensive agricultural land use. Ecol. Evol. 5, 2556–2571. https://doi.org/10.1002/ece3.1534.

Izquieta-Rojano, S., García-Gomez, H., Aguillaume, L., Santamaría, J.M., Tang, Y.S., Santamaría, C., Valiño, F., Lasheras, E., Alonso, R., Àvila, A., Cape, J.N., Elustondo, D., 2016. Throughfall and bulk deposition of dissolved organic nitrogen to holm oak forests in the Iberian Peninsula: flux estimation and identification of potential sources. Environ. Pollut. 210, 104–112. https://doi.org/10.1016/j.envpol.2015.12.002.

Jiang, C.M., Yu, W.T., Ma, Q., Xu, Y.G., Zou, H., Zhang, S.C., Sheng, W.P., 2013. Atmospheric organic nitrogen deposition: analysis of nationwide data and a case study in Northeast China. Environ. Pollut. 182, 430–436. https://doi.org/10.1016/j.envpol.2013.08.003.

Jickells, T., Baker, A.R., Cape, J.N., Cornell, S.E., Nemitz, E., 2013. The cycling of organic nitrogen through the atmosphere. Philos. Trans. R. Soc. B 368, 20130115. https://doi.org/10.1098/rstb.2013.0115.

Johansson, O., Nordin, A., Olofsson, J., Palmqvist, K., 2010. Responses of epophytic lichens to an experimental whole-tree nitrogen-deposition gradient. New Phytol. 188, 1075–1084.

Kang, Y., Liu, M., Song, Y., Huang, X., Yao, H., Cai, X., Zhang, H., Kang, L., Liu, X., Yan, X., He, H., Zhang, Q., Shao, M., Zhu, T., 2016. High-resolution ammonia emissions inventories in China from 1980 to 2012. Atmos. Chem. Phys. 16, 2043–2058. https://doi.org/10.5194/acp-16-2043-2016.

Ke, P.P., Yu, Q., Luo, Y., Kang, R.H., Duan, L., 2020. Fluxes of nitrogen oxides above a subtropical forest canopy in China. Sci. Total Environ. 715, 138993.

Kjnaas, O.J., 1999. In situ efficiency of ion exchange resins in studies of nitrogen transformation. Soil Sci. Soc. Am. J. 63, 399–409. https://doi.org/10.2136/sssaj1999.03615995006300020019x.

Kuang, F., Liu, X., Zhu, B., Shen, J., Pan, Y., Su, M., Goulding, K., 2016. Wet and dry nitrogen deposition in the central Sichuan Basin of China. Atmos. Environ. 143, 39–50. https://doi.org/10.1016/j.atmosenv.2016.08.032.

Kuik, F., Lauer, A., Churkina, G., Denier van der Gon, H.A.C., Fenner, D., Mar, K.A., Butler, T.M., 2016. Air quality modelingin the Berlin–Brandenburg region using WRF-Chem v3.7.1: sensitivity to resolution of model grid and input data. Geosci. Model Dev. 9, 4339–4363. https://doi.org/10.5194/gmd-9-4339-2016.

Lee, D.S., Longhurst, J.W.S., 1992. A comparison between wet and bulk deposition at an urban site in the U.K. Water Air Soil Pollut. 1992 (64), 635–648. https://doi.org/10.1007/BF00483372.

Lichiheb, N., Myles, L., Personne, E., Heuer, M., Buban, M., Nelson, A.J., Koloutsou-Vakakis, S., Rood, M.J., Joo, E., Miller, J., Bernacchi, C., 2019. Implementation of the effect of urease inhibitor on ammonia emissions following urea-based fertilizer application at a Zea mays field in central Illinois: a study with SURFATM-NH_3 model. Agr. For. Meteorol. 269–270, 78–87. https://doi.org/10.1016/j.agrformet.2019.02.005.

Liu, X.J., Du, E.Z., 2020. Part I: Reactive Nitrogen Emission and Deposition in China. Springer. https://doi.org/10.1007/978-981-13-8514-8.

Liu, M.X., Huang, X., Song, Y., Tang, J., Cao, J.J., Zhang, X.Y., Zhang, Q., Wang, S.X., Xu, T.T., Kang, L., Cai, X.H., Zhang, H.S., Yang, F.M., Wang, H.B., Yu, J.Z., Lau, A.K. H., He, L.Y., Huang, X.F., Duan, L., Ding, A.J., Xue, L.K., Liu, B., Zhu, T., 2019. Ammonia emission control in China would mitigate haze pollution and nitrogen deposition, but worsen acid rain. Proc. Natl. Acad. Sci. U. S. A. 116, 7760–7765. https://doi.org/10.1073/pnas.1814880116.

Liu, H.Y., Jacob, D.J., Bey, I., Yantosca, R.M., 2001. Constraints from Pb-210 and Be-7 on wet deposition and transport in a global three-dimensional chemical tracer model driven by assimilated meteorological fields. J. Geophys. Res. -Atmos. 106, 12109–12128. https://doi.org/10.1088/1748-9326/11/11/114002.

Liu, X.Y., Xiao, H.Y., Liu, C.Q., Li, Y.Y., Xiao, H.W., 2008. Stable carbon and nitrogen isotopes of the moss *Haplocladium microphyllum* in an urban and a background area (SW China): the role of environmental conditions and atmospheric nitrogen deposition. Atmos. Environ. 42, 5413–5423. https://doi.org/10.1016/j.atmosenv.2008.02.038.

Liu, X.J., Xu, W., Duan, L., Du, E.Z., Pan, Y.P., Lu, X.K., Zhang, L., Wu, Z.Y., Wang, X.M., Zhang, Y., Shen, J.L., Song, L., Feng, Z.Z., Liu, X.Y., Song, W., Tang, A.H., Zhang, Y. Y., Zhang, X.Y., Collett Jr., J.L., Chang, Y.H., 2017e. Atmospheric nitrogen emission, deposition and air quality impacts in China: an overview. Curr. Pollut. Rep. 3, 65–77. https://doi.org/10.1007/s40726-017-0056-6.

Liu, X.J., Xu, W., Pan, Y.P., Du, E.Z., 2015. Liu et al. suspect that Zhu et al. (2015) may have underestimated dissolved organic nitrogen (N) but overestimated total particulate N in wet deposition in China. Sci. Total Environ. 520, 300–301. https://doi.org/10.1016/j.scitotenv.2015.03.004.

Liu, F., Zhang, Q., van der, A., Zheng, R.J., Tong, B., Yan, D., Zheng, L., He, K.B, Y.X., 2016. Recent reduction in NO_x emissions over China: synthesis of satellite observations and emission inventories. Environ. Res. Lett. 11, 114002 https://doi.org/10.1088/1748-9326/11/11/114002.

Liu, L., Zhang, X., Xu, W., Liu, X., Li, Y., Lu, X., Zhang, Y., Zhang, W., 2017a. Temporal characteristics of atmospheric ammonia and nitrogen dioxide over China based on emission data, satellite observations and atmospheric transport modelingsince 1980. Atmos. Chem. Phys. 17, 1–32. https://doi.org/10.5194/acp-17-9365-2017.

Liu, L., Zhang, X.Y., Xu, W., Liu, X.J., Lu, X., Chen, D.M., Zhang, X.M., Wang, S.Q., Zhang, W.T., 2017b. Estimation of monthly bulk nitrate deposition in China based on satellite NO_2 measurement by the Ozone Monitoring Instrument. Remote Sens. Environ. 199, 93–106. https://doi.org/10.1016/j.rse.2017.07.005.

Liu, L., Zhang, X.Y., Xu, W., Liu, X.J., Lu, X.H., Wang, S.Q., Zhang, W.T., Zhao, L.M., 2017c. Ground ammonia concentrations over china derived from satellite and atmospheric transport modeling. Remote Sens. 9, 467. https://doi.org/10.3390/rs9050467.

Liu, L., Zhang, X., Xu, W., Liu, X., Lu, X., Wei, J., Li, Y., Yang, Y., Wang, Z., Wong, A.Y.H., 2020a. Reviewing global estimates of surface reactive nitrogen concentration and deposition using satellite observation. Atmos. Chem. Phys. 20, 8641–8658. https://doi.org/10.5194/acp-20-8641-2020.

Liu, L., Zhang, X.Y., Xu, W., Liu, X.J., Wei, J., Wang, Z., Yang, Y.Y., 2020b. Global estimates of dry ammonia deposition inferred from space-measurements. Sci. Total Environ. 730, 139189 https://doi.org/10.1016/j.scitotenv.2020.139189.

Liu, L., Zhang, X.Y., Zhang, Y., Xu, W., Liu, X.J., Zhang, X.M., Feng, J.L., Chen, X.R., Zhang, Y.H., Lu, X.H., Wang, S.Q., Zhang, W.T., Zhao, L.M., 2017d. Dry particulate nitrate deposition in China. Environ. Sci. Technol. 51, 5572–5581. https://doi.org/10.1021/acs.est.7b00898.

Li, Y., Schichtel, B.A., Walker, J.T., Schwede, D.B., Chen, X., Lehmann, C.M.B., Puchalski, M.A., Gay, D.A., Collett, J.L., 2016. Increasing importance of deposition of reduced nitrogen in the United States. Proc. Natl. Acad. Sci. U. S. A. 116, 8657–8666. https://doi.org/10.1073/pnas.1525736113.

Lu, X.K., Mao, Q.G., Gilliam, F.S., Luo, Y.Q., Mo, J.M., 2014. Nitrogen deposition contributes to soil acidification in tropical ecosystems. Glob. Change Biol. 20, 3790–3801. https://doi.org/10.1111/gcb.12665.

Massad, R.S., Nemitz, E., Sutton, M.A., 2010. Review and parameterisation of bidirectional ammonia exchange between vegetation and the atmosphere. Atmos. Chem. Phys. 10, 10359–10386. https://doi.org/10.5194/acp-10-10359-2010.

McMurray, J.A., Roberts, D.W., Fenn, M.E., Geiser, L.H., Jovan, S., 2013. Using epiphytic lichens to monitor nitrogen deposition near natural gas drilling operations in the Wind River Range, WY, USA. Water Air Soil Pollut. 224, 1487. https://doi.org/10.1007/s11270-013-1487-3.

McMurray, J.A., Roberts, D.W., Geiser, L.H., 2015. Epiphytic lichen indication of nitrogen deposition and climate in the northern rocky mountains, USA. Ecol. Indic. 49, 154–161. https://doi.org/10.1016/j.ecolind.2014.10.015.

Mehlert, S., Schmidt, G., Russow, R., 1995. Measuring of the integral airborne nitrogen-input into a soil-plat system by the ^{15}N-isotope dilution method. Isot. Environ. Health Stud. 31, 377–383. https://doi.org/10.1080/10256019508036285.

Midolo, G., Alkemade, R., Schipper, A.M., Benítez-López, A., Perring, M.P., De Vries, W., 2019. Impacts of nitrogen addition on plant species richness and abundance: a global meta-analysis. Glob. Ecol. Biogeogr. 28, 398–413. https://doi.org/10.1111/geb.12856.

Miller, D.J., Sun, K., Tao, L., Khan, M.A., Zondlo, M.A., 2014. Open-path, quantum cascade-laser-based sensor for high-resolution atmospheric ammonia measurements. Atmos. Meas. Tech. 7, 81–93. https://doi.org/10.5194/amt-7-81-2014.

Miyazaki, K., Eskes, H., Sudo, K., Boersma, K.F., Bowman, K., Kanaya, Y., 2017. Decadal changes in global surface NO_x emissions from multi-constituent satellite data assimilation. Atmos. Chem. Phys. 17, 807–837. https://doi.org/10.5194/acp-17-807-2017.

Mizak, C.A., Campbell, S.W., Luther, M.E., Carnahan, R.P., Murphy, R.J., Poor, N.D., 2005. Below-cloud ammonia scavenging in convective thunderstorms at a coastal research site in Tampa, FL, USA. Atmos. Environ. 39, 1575–1584. https://doi.org/10.1016/j.atmosenv.2004.10.008.

Munzi, S., Branquinho, C., Cruz, C., Máguas, C., Leith, I.D., Sheppard, L.J., Sutton, M.A., 2019. $\delta^{15}N$ of lichens reflects the isotopic signature of ammonia source. Sci. Total Environ. 653, 698–704. https://doi.org/10.1016/j.scitotenv.2018.11.010.

Nadim, F., Trahiotis, M.M., Stapcinskaite, S., Perkins, C., Carley, R.J., Hoag, G.E., Yang, X.S., 2001. Estimation of wet, dry and bulk deposition of atmospheric nitrogen in Connecticut. J. Environ. Monit. 3, 671–680. https://doi.org/10.1039/B107008H.

Neff, J.C., Holland, E.A., Dentener, F.J., McDowell, W.H., Russell, K.M., 2002. The origin, composition and rates of organic nitrogen deposition: a missing piece of nitrogen cycle? Biogeochemistry 57/58 (1), 99–136. https://doi.org/10.1023/A:1015791622742.

Neirynck, J., Kowalski, A.S., Carrara, A., Genouw, G., Berghmans, P., Ceulemans, R., 2007. Fluxes of oxidised and reduced nitrogen above a mixed coniferous forest exposed to various nitrogen emission sources. Environ. Pollut. 149, 31–43. https://doi.org/10.1016/j.envpol.2006.12.029.

Nelson, A.J., Koloutsou-Vakakis, S., Rood, M.J., Myles, L., Lehmann, C., Bernacchi, C., Balasubrammanian, S., Joo, E., Heuer, M., Vieira-Filho, M., Lin, J., 2017. Season-long ammonia flux measurements above fertilized corn in central Illinois, USA, using relaxed eddy accumulation. Agr. For. Meteorol. 239, 202–212. https://doi.org/10.1016/j.agrformet.2017.03.010.

Nemitz, E., Milford, C., Sutton, M.A., 2001. A two-layer canopy compensation point model for describing bi-directional biosphere- atmosphere exchange of ammonia. Q. J. R. Meteorol. Soc. 127, 815–833. https://doi.org/10.1002/qj.49712757306.

Nemitz, E., Sutton, M.A., Schjoerring, J.K., Husted, S., Wyers, G.P., 2000. Resistance modelingof ammonia exchange over oilseed rape. Agr. For. Meteorol. 105, 405–425. https://doi.org/10.1016/S0168-1923(00)00206-9.

Nemitz, E., Sutton, M.A., Wyers, G.P., Jongejan, P.A.C., 2004. Gas-particle interactions above a Dutch heathland: I. Surface exchange fluxes of NH_3, SO_2, HNO_3 and HCl. Atmos. Chem. Phys. 4, 989–1005. https://doi.org/10.5194/acp-4-989-2004.

Ochoa-Hueso, R., Allen, E.B., Branquinho, C., Cruz, C., Dias, T., Fenn, M.E., Manrique, E., Pérez-Corona, M.E., Sheppard, L.J., Stock, W.D., 2011. Nitrogen deposition effects on Mediterranean-type ecosystems: an ecological assessment. Environ. Pollut. 159, 2265–2279.

Oishi, Y., 2019. Moss as an indicator of transboundary atmospheric nitrogen pollution in an alpine ecosystem. Atmos. Environ. 208, 158–166. https://doi.org/10.1016/j.atmosenv.2019.04.005.

Pan, Y.P., Wang, Y.S., Tang, G.Q., Wu, D., 2012. Wet and dry deposition of atmospheric nitrogen at ten sites in Northern China. Atmos. Chem. Phys. 12, 6515–6535. https://doi.org/10.5194/acp-12-6515-2012.

Phillips, S.B., Arya, S.P., Aneja, V.P., 2004. Ammonia flux and dry deposition velocity from near-surface concentration gradient measurements over a grass surface in North Carolina. Atmos. Environ. 38, 3469–3480. https://doi.org/10.1016/j.atmosenv.2004.02.054.

Pinho, P., Barros, C., Augusto, A., Pereira, M.J., Máguas, C., Branquinha, C., 2017. Using nitrogen concentration and isotopic composition in lichens to spatially assess the relative contribution of atmospheric nitrogen sources in complex landscapes. Environ. Pollut. 230, 632–638. https://doi.org/10.1016/j.envpol.2017.06.102.

Qiao, X., Tang, Y., Hu, J.L., Zhang, S., Li, J.Y., Kota, S.H., Wu, L., Gao, H.L., Zhang, H.L., Ying, Q., 2015. Modelingdry and wet deposition of sulfate, nitrate, and ammonium ions in Jiuzhaigou National Nature Reserve, China using a source-oriented CMAQ

model: Part I. Base case model results. Sci. Total Environ. 532, 831–839. https://doi.org/10.1016/j.scitotenv.2015.05.108.
Qu, L.L., Xiao, H.Y., Guan, H., Zhang, Z.Y., Xu, Y., 2016. Total N content and $\delta^{15}N$ signatures in moss tissue for indicating varying atmospheric nitrogen deposition in Guizhou Province, China. Atmos. Environ. 142, 145–151. https://doi.org/10.1016/j.atmosenv.2016.07.044.
Root, H.T., Geiser, L.H., Fenn, M.E., Jovan, S., Hutten, M.A., Ahuja, S., Dillman, K., Schirokauer, D., Berryman, S., McMurray, J.A., 2013. A simple tool for estimating throughfall nitrogen deposition in forests of western North America using lichens. For. Ecol. Manag. 306, 1–8. https://doi.org/10.1016/j.foreco.2013.06.028.
Root, H.T., Geiser, L.H., Jovan, S., Neitlich, P., 2015. Epiphytic macrolichen indication of air quality and climate in interior forested mountains of the Pacific northwest, USA. Ecol. Indic. 53, 95–105. https://doi.org/10.1016/j.ecolind.2015.01.029.
Russow, R., Böhme, F., 2005. Determination of the total nitrogen deposition by the N-15 isotope dilution method and problems in extrapolating results to field scale. Geoderma 127, 62–70. https://doi.org/10.1016/j.geoderma.2004.11.015.
Saki, H., Goudarzi, G., Jalali, S., Barzegar, G., Farhadi, M., Parseh, I., Geravandi, S., Salmanzadeh, S., Yousefi, F., Mohammadi, M.J., 2019. Study of relationship between nitrogen dioxide and chronic obstructive pulmonary disease in Bushehr, Iran. Clin. Epidemiol. Glob. Health 8, 446–449. https://doi.org/10.1016/j.cegh.2019.10.006.
Salemaa, M., Mäkipää, R., Oksanen, J., 2008. Differences in the growth response of three bryophyte species to nitrogen. Environ. Pollut. 152, 82–91. https://doi.org/10.1016/j.envpol.2007.05.019.
Schmitz, A., Sanders, T.G., Bolte, A., Bussotti, F., Dirnböck, T., Johnson, J., Peñuelas, J., Pollastrini, M., Prescher, A.-K., Sardans, J., Verstraeten, A., de Vries, W., 2019. Responses of forest ecosystems in Europe to decreasing nitrogen deposition. Environ. Pollut. 244, 980–994. https://doi.org/10.1016/j.envpol.2018.09.101.
Schröder, W., Pesch, R., Schönrock, S., Harmens, H., Mills, G., Fagerli, H., 2014. Mapping correlations between nitrogen concentrations in atmospheric deposition and mosses for natural landscapes in Europe. Ecol. Indic. 36, 563–571. https://doi.org/10.1016/j.ecolind.2013.09.013.
Seinfeld, J.H., Pandis, S.N., 2006. Atmospheric Chemistry and Physics: From Air Pollution to Climate Change, 2nd ed. Wiley Interscience, New Jersey. https://doi.org/10.1063/1.882420.
Shen, J.L., Li, Y., Liu, X.J., Luo, X.S., Tang, H., Zhang, Y.Z., Wu, J.S., 2013. Atmospheric dry and wet nitrogen deposition on three contrasting land use types of an agricultural catchment in subtropical central China. Atmos. Environ. 67, 415–424. https://doi.org/10.1016/j.atmosenv.2012.10.068.
Sickman, J.O., James, A.E., Fenn, M.E., Bytnerowicz, A., Lucero, D.M., Homyak, P.M., 2019. Quantifying atmospheric N deposition in dryland ecosystems: a test of the Integrated Total Nitrogen Input (ITNI) method. Sci. Total Environ. 646, 1253–1264. https://doi.org/10.1016/j.scitotenv.2018.07.320.
Slinn, W.G.N., 1982. Predictions for particle deposition to vegetative surfaces. Atmos. Environ. 16, 1785–1794. https://doi.org/10.1016/0004-6981(82)90271-2.
Smith, B.J., Nitschke, M., Pilotto, L.S., Ruffin, R.E., Pisaniello, D.L., Willson, K.J., 2000. Health effects of daily indoor nitrogen dioxide exposure in people with asthma. Eur. Respir. J. 16, 879–885. https://doi.org/10.1183/09031936.00.16587900.
Solga, A., Burkhardt, J., Zechmeister, H.G., Frahm, J.P., 2005. Nitrogen content, ^{15}N natural abundance and biomass of the two pleurocarpous mosses *Pleurozium schreberi* (Brid.) Mitt and *Scleropodium purum* (Hedw.) Limpr. in relation to atmospheric nitrogen deposition. Environ. Pollut. 134, 465–473. https://doi.org/10.1016/j.envpol.2004.09.008.
Sommar, J., Zhu, W., Shang, L., Feng, X., Lin, C.J., 2013. A whole-air relaxed eddy accumulation measurement system for sampling vertical vapour exchange of elemental mercury. Tellus B: Chem. Phys. Meteorol. 65, 19940. https://doi.org/10.3402/tellusb.v65i0.19940.
Sommer, S.G., 1988. A simple biomonitor for measuring ammonia deposition in rural areas. Biol. Fertil. Soils 6, 61–64. https://doi.org/10.1007/BF00257922.
Song, L., Kuang, F.H., Skiba, U., Zhu, B., Liu, X.J., Levy, P., Dore, A.J., Fowler, D., 2017. Bulk deposition of organic and inorganic nitrogen in southwest China from 2008 to 2013. Environ. Pollut. 227, 157–166. https://doi.org/10.1016/j.envpol.2017.04.031.
Staelens, J., De Schrijver, A., Van Avermaet, P., Genouw, G., Verhoest, N., 2005. A comparison of bulk and wet-only deposition at two adjacent sites in Melle (Belgium). Atmos. Environ. 39, 7–15. https://doi.org/10.1016/j.atmosenv.2004.09.055.
Stevens, C.J., Dupre, C., Dorland, E., Gaudnik, C., Gowing, D.J.G., Bleeker, A., Diekmann, M., Alard, D., Bobbink, R., Fowler, D., Corcket, E., Mountford, J.O., Vandvik, V., Aarrestad, P.A., Muller, S., Dise, N.B., 2011. The impact of nitrogen deposition on acid grasslands in the Atlantic region of Europe. Environ. Pollut. 159, 2243–2250. https://doi.org/10.1016/j.envpol.2010.11.026.
Sun, K., Tao, L., Miller, D.J., Zondlo, M.A., Shonkwiler, C.N., Nash, C., Ham, J.M., 2015. Open-path eddy covariance measurements of ammonia fluxes from a beef cattle feedlot. Agr. For. Meteorol. 213, 193–202. https://doi.org/10.1016/j.agrformet.2015.06.007.
Sutton, M.A., Burkhardt, J.K., Guerin, D., Nemitz, E., Fowler, D., 1998. Development of resistance models to describe measurements of bi-directional ammonia surface-atmosphere exchange. Atmos. Environ. 32, 473–480. https://doi.org/10.1016/S1352-2310(97)00164-7.
Sutton, M.A., Milford, C., Nemitz, E., Theobald, M.R., Hill, P.W., Fowler, D., Schjoerring, J.K., Mattsson, M.E., Nielsen, K.H., Husted, S., Erisman, J.W., Otjes, R., Hensen, A., Mosquera, J., Cellier, P., Loubet, B., David, M., Genermont, S., Neftel, A., Blatter, A., Herrmann, B., Jones, S.K., Horvath, L., Fuhrer, E.C., Mantzanas, K., Koukoura, Z., Gallagher, M., Williams, P., Flynn, M., Riedo, M., 2001. Biosphere-atmosphere interactions of ammonia with grasslands: experimental strategy and results from a new European initiative. Plant Soil 1, 131–145. https://doi.org/10.1023/A:1004822100016.
Tang, Y.S., Simmons, I., van Dijk, N., Di Marco, C., Nemitz, E., Dammgen, U., Gilke, K., Djuricic, V., Vidic, S., Gliha, Z., 2009. European scale application of atmospheric reactive nitrogen measurements in a low-cost approach to infer dry deposition fluxes. Agr. Ecosyst. Environ. 133, 183–195. https://doi.org/10.1016/j.agee.2009.04.027.
Tan, J., Fu, J.S., Dentener, F., Sun, J., Emmons, L., Tilmes, S., Sudo, K., Flemming, J., Jonson, J.E., Gravel, S., Bian, H., Davila, Y., Henze, D.K., Lund, M.T., Kucsera, T., Takemura, T., Keating, T., 2018. Multi-model study of HTAP II on sulfur and nitrogen deposition. Atmos. Chem. Phys. 18, 6847–6866. https://doi.org/10.5194/acp-18-6847-2018.
Tan, J.N., Fu, J.S., Seinfeld, J.H., 2020. Ammonia emission abatement does not fully control reduced forms of nitrogen deposition. Proc. Natl. Acad. Sci. U. S. A. 117, 9771–9775. https://doi.org/10.1073/pnas.1920068117.
Tørseth, K., Aas, W., Breivik, K., Fjæraa, A.M., Fiebig, M., Hjellbrekke, A.G., Lund Myhre, C., Solberg, S., Yttri, K.E., 2012. Introduction to the European Monitoring and Evaluation Programme (EMEP) and observed atmospheric composition change during 1972–2009. Atmos. Chem. Phys. 12, 5447–5481. https://doi.org/10.5194/acp-12-5447-2012.
Vet, R., Artz, R.S., Carou, S., Shaw, M., Ro, C.-U., Aas, W., Baker, A., Bowersox, V.C., Dentener, F., Galy-Lacaux, C., Hou, A., Pienaar, J.J., Gillett, R., Forti, M.C., Gromov, S., Hara, H., Khodzher, T., Mahowald, N.M., Nickovic, S., Rao, P.S.P., Reid, N.W., 2014. A global assessment of precipitation chemistry and deposition of sulfur, nitrogen, sea salt, base cations, organic acids, acidity and pH, and phosphorus. Atmos. Environ. 93, 3–100. https://doi.org/10.1016/j.atmosenv.2013.10.060.
Wang, H.B., Shi, G.M., Tian, M., Chen, Y., Qiao, B.Q., Zhang, L.Y., Yang, F.M., Zhang, L.M., Luo, Q., 2018. Wet deposition and sources of inorganic nitrogen in the Three Gorges Reservoir Region, China. Wet deposition and sources of inorganic nitrogen in the Three Gorges Reservoir Region, China. Environ. Pollut. 233, 520–528. https://doi.org/10.1016/j.envpol.2017.10.085.
Weigel, A., Russow, R., Korschens, M., 2000. Quantification of airborne N-input in longterm field experiments and its validation through measurements using ^{15}N isotope dilution. J. Plant Nutr. Soil Sci. 163, 261–265. https://doi.org/10.1002/1522-2624(200006)163:33.0.CO;2-M.
Wen, Z., Xu, W., Li, Q., Han, M.J., Tang, A.H., Zhang, Y., Luo, X.S., Shen, J.L., Wang, W., Li, K.H., Pan, Y.P., Zhang, L., Li, W.Q., Collett Jr., J.L., Zhong, B.Q., Wang, X.M., Goulding, K., Zhang, F.S., Liu, X.J., 2020. Changes of nitrogen deposition in China from 1980 to 2018. Environ. Int. 144, 106022 https://doi.org/10.1016/j.envint.2020.106022.
Wesely, M.L., Hicks, B.B., 1977. Some factors that affect the deposition rates of sulfur dioxide and similar gases on vegetation. J. Air Pollut. Control Assoc. 27, 1110–1116. https://doi.org/10.1080/00022470.1977.10470534.
Wesely, M.L., 1989. Parameterization of surface resistances to gaseous dry deposition in regional-scale numerical-models. Atmos. Environ. 23, 1293–1304. https://doi.org/10.1016/j.atmosenv.2007.10.058.
Wesely, M.L., Hicks, B.B., 2000. A review of the current status of knowledge on dry deposition. Atmos. Environ. 34, 2261–2282. https://doi.org/10.1016/S1352-2310(99)00467-7.
Whaley, C., Makar, P.A., Shephard, M.W., Zhang, L.M., Zhang, J.H., Zheng, Q., Akingunola, A., Wentworth, G.R., Murphy, J.G., Kharol, S.K., Cady-Pereira, K.E., 2018. Contributions of natural and anthropogenic sources to ambient ammonia in the Athabasca Oil Sands and north-western Canada. Atmos. Chem. Phys. 18, 2011–2034. https://doi.org/10.5194/acp-18-2011-2018.
Wolff, V., Trebs, I., Ammann, C., Meixner, F.X., 2010. Aerodynamic gradient measurements of the NH3-HNO3-NH4NO3 triad using a wet chemical instrument: an analysis of precision requirements and flux errors. Atmos. Meas. Tech. 3, 187–208. https://doi.org/10.5194/amt-3-187-2010.
Xiao, H.Y., Tang, C.G., Xiao, H.W., Liu, X.Y., Liu, C.Q., 2010. Mosses indicating atmospheric nitrogen deposition and sources in the Yangtze River drainage basin, China. J. Geophys. Res. 115, D14301 https://doi.org/10.1029/2009JD012900.
Xiao, H.Y., Xie, Z.Y., Tang, C.G., Wang, Y.L., Liu, C.Q., 2011. Epilithic moss as a bio-monitor of atmospheric N deposition in South China. J. Geophys. Res. 116, n/a–n/a. https://doi.org/10.1029/2011JD016229.
Xu, W., Liu, L., Cheng, M., Zhao, Y., Zhang, L., Pan, Y., Zhang, X., Gu, B., Li, Y., Zhang, X., Shen, J., Lu, L., Luo, X., Zhao, Y., Feng, Z., Collett Jr., J.L., Zhang, F., Liu, X., 2018. Spatial–temporal patterns of inorganic nitrogen air concentrations and deposition in eastern China. Atmos. Chem. Phys. 18, 10931–10954. https://doi.org/10.5194/acp-18-10931-2018.
Xu, W., Luo, X.S., Pan, Y.P., Zhang, L., Tang, A.H., Shen, J.L., Zhang, Y., Li, K.H., Wu, Q.H., Yang, D.W., Zhang, Y.Y., Xue, J., Li, W.Q., Li, Q.Q., Tang, L., Lu, S.H., Liang, T., Tong, Y.A., Liu, P., Zhang, Q., Xiong, Z.Q., Shi, X.J., Wu, L.H., Shi, W.Q., Tian, K., Zhong, X.H., Shi, K., Tang, Q.Y., Zhang, L.J., Huang, J.L., He, C.E., Kuang, F.H., Zhu, B., Liu, H., Jin, X., Xin, Y.J., Shi, X.K., Du, E.Z., Dore, A.J., Tang, S., Collett Jr., J.L., Goulding, K., Sun, Y.X., Ren, J., Zhang, F.S., Liu, X.J., 2015. Quantifying atmospheric nitrogen deposition through a nationwide monitoring network across China. Atmos. Chem. Phys. 15, 12345–12360. https://doi.org/10.5194/acp-15-12345-2015.
Xu, W., Zhang, L., Liu, X., 2019. A database of atmospheric nitrogen concentration and deposition from the nationwide monitoring network in China. Sci. Data 6, 51. https://doi.org/10.1038/s41597-019-0061-2.
Xu, W., Zhao, Y.H., Liu, X.J., Dore, A.J., Zhang, L., Liu, L., Cheng, M.M., 2018a. Atmospheric nitrogen deposition in the Yangtze River basin: Spatial pattern and source attribution. Environ. Pollut. 232, 546–555.

Yu, G., Jia, Y., He, N., Zhu, J., Chen, Z., Wang, Q., Piao, S., Liu, X., He, H., Guo, X., 2019. Stabilization of atmospheric nitrogen deposition in China over the past decade. Nat. Geosci. 12, 424–429. https://doi.org/10.1038/s41561-019-0352-4.

Zhang, L.M., Brook, J.R., Vet, R., 2003. A revised parameterization for gaseous dry deposition in air-quality models. Atmos. Chem. Phys. 3, 2067–2082. https://doi.org/10.5194/acp-3-2067-2003.

Zhang, L., Chen, Y., Zhao, Y., Henze, D.K., Zhu, L., Song, Y., Paulot, F., Liu, X., Pan, Y., Lin, Y., Huang, B., 2018. Agricultural ammonia emissions in China: reconciling bottom-up and top-down estimates. Atmos. Chem. Phys. 18, 339–355. https://doi.org/10.5194/acp-18-339-2018.

Zhang, L.M., Gong, S.L., Padro, J., Barrie, L., 2001. A size-segregated particle dry deposition scheme for an atmospheric aerosol module. Atmos. Environ. 35, 549–560. https://doi.org/10.1016/S1352-2310(00)00326-5.

Zhang, Y., Liu, X.J., Fangmeier, A., Goulding, K.T.W., Zhang, F.S., 2008. Nitrogen inputs and isotopes in precipitation in the North China Plain. Atmos. Environ. 42, 1436–1448.

Zhang, L.M., Might, L.P., Asman, W.A.H., 2010. Bi-directional airsurface exchange of atmospheric ammonia: a review of measurements and a development of a big-leaf model for applications in regional-scale air-quality models. J. Geophys. Res. 115, D20310 https://doi.org/10.1029/2009JD013589.

Zhang, Y., Song, L., Liu, X.J., Li, W.Q., Lü, S.H., Zheng, L.X., Bai, Z.C., Cai, G.Y., Zhang, F. S., 2012. Atmospheric organic nitrogen deposition in China. Atmos. Environ. 46, 195–204. https://doi.org/10.1016/j.atmosenv.2011.09.080.

Zhan, X., Bo, Y., Zhou, F., Liu, X., Paerl, H.W., Shen, J., Wang, R., Li, F., Tao, S., Dong, Y., 2017. Evidence for the importance of atmospheric nitrogen deposition to eutrophic lake Dianchi, China. Environ. Sci. Technol. 51, 6699–6708. https://doi.org/10.1021/acs.est.6b06135.

Zhao, Y., Zhang, L., Chen, Y.F., Liu, X.J., Xu, W., Pan, Y.P., Duan, L., 2017. Atmospheric nitrogen deposition to China: a model analysis on nitrogen budget and critical load exceedance. Atmos. Environ. 153, 32–40. https://doi.org/10.1016/j.atmosenv.2017.01.018.

Zheng, X.D., Liu, X.Y., Song, W., Sun, X.C., Liu, C.Q., 2018. Nitrogen isotope variations of ammonium across rain events: implications for different scavenging between ammonia and particulate ammonium. Environ. Pollut. 239, 392–398. https://doi.org/10.1016/j.envpol.2018.04.015.

Zheng, B., Tong, D., Li, M., Liu, F., Hong, C., Geng, G., Li, H., Li, X., Peng, L., Qi, J., Yan, L., Zhang, Y., Zhao, H., Zheng, Y., He, K., Zhang, Q., 2018. Trends in China's anthropogenic emissions since 2010 as the consequence of clean air actions. Atmos. Chem. Phys. 18, 14095–14111. https://doi.org/10.5194/acp-2018-374.

Zhu, J.X., He, N.P., Wang, Q.F., Yuan, G.F., Wen, D., Yu, G.R., Jia, Y.L., 2015. The composition, spatial patterns, and influencing factors of atmospheric wet nitrogen deposition in Chinese terrestrial ecosystems. Sci. Total Environ. 511, 777–785. https://doi.org/10.1016/j.scitotenv.2014.12.038.